

Efficient Detection of Strong-To-Weak Spontaneous Symmetry Breaking via the Rényi-1 Correlator

Zack Weinstein*

Department of Physics, University of California, Berkeley, CA 94720, USA

(Dated: November 1, 2024)

Strong-to-weak spontaneous symmetry breaking (SWSSB) has recently emerged as a universal feature of quantum mixed-state phases of matter. While various information-theoretic diagnostics have been proposed to define and characterize SWSSB phases, relating these diagnostics to observables which can be efficiently and scalably probed on modern quantum devices remains challenging. Here we propose a new observable for SWSSB in mixed states, called the *Rényi-1 correlator*, which naturally suggests a potential route towards scalably detecting SWSSB phases in experiment. Specifically, if the *canonical purification* (CP) of a given mixed state can be reliably prepared, then SWSSB in the mixed state can be detected via ordinary two-point correlation functions in the CP state. We discuss several simple examples of CP states which can be efficiently prepared on quantum devices, and whose reduced density matrices exhibit SWSSB. The Rényi-1 correlator also satisfies several useful theoretical properties: it naturally inherits a stability theorem recently proven for the closely-related fidelity correlator, and it directly defines SWSSB as a particular pattern of ordinary spontaneous symmetry breaking in the CP state.

There has recently been an explosion of interest in characterizing and classifying mixed-state phases of quantum matter. Whereas the study of quantum phases has previously been largely restricted to quantum ground states or to thermal Gibbs states [1, 2], experimental advances in quantum simulation [3–8], quantum state preparation [9–12], and quantum error correction [13–15] have motivated the study of a new class of “locally decohered” mixed states [16–20]. In turn, these states have revealed fresh theoretical insights on the relation between mixed-state topological order and quantum error correction [21–29], on new classifications of topological and symmetry-protected topological phases in mixed states [30–36], and on the very notion of what constitutes a mixed-state phase of matter [37–41].

Traditionally, the most important characterization of both classical and quantum phases is how they manifest their symmetries [42, 43]. While a pure state can only be symmetric or non-symmetric under a symmetry transformation, mixed states can be symmetric in one of two distinct senses: mixed states with a single well-defined symmetry charge are said to exhibit a “strong” symmetry, while mixed states composed of an incoherent mixture of symmetry charges exhibit only a “weak” symmetry, that is, they are only symmetric “on average”. Curiously, there is a sense in which a mixed state’s strong symmetry can be spontaneously broken *without* breaking the corresponding weak symmetry [19]. This phenomenon, recently dubbed *strong-to-weak spontaneous symmetry breaking* (SWSSB) [19, 44–47], serves as a new universal characterization of phases of quantum matter which is unique to mixed states.

A crucial feature of SWSSB which distinguishes it from conventional spontaneous symmetry breaking (SSB) is that its defining observables are necessarily information-theoretic. In order for the weak symmetry to remain

unbroken, ordinary two-point correlation functions of operators charged under the broken strong symmetry must remain short-range ordered. In place of these conventional observables, SWSSB has previously been defined by diagnostics such as the Rényi-2 correlator [19, 45] and the fidelity correlator [44] (to be defined below), which measure the *distinguishability* between a mixed state ρ and the same state with added symmetry charges. While these diagnostics both have several theoretically appealing features, they are also highly nonlinear in ρ , and consequently they are extraordinarily difficult to measure in experiment. As a result, the practical implications of SWSSB on observable features of mixed states in modern quantum devices have remained unclear.

In this Letter, we put forth a new observable for SWSSB called the *Rényi-1 correlator*, denoted $R_1(x, y)$ below, which exhibits several theoretically and practically useful features. Whereas the Rényi-2 correlator is defined by treating ρ as a pure state in a doubled Hilbert space, R_1 is defined in a doubled Hilbert space via two-point correlations in the *canonical purification* (CP) of ρ . Consequently, while R_1 exhibits much of the same useful symmetry properties of the Rényi-2 correlator, it also shares important information-theoretic features with the fidelity correlator. Specifically, R_1 directly inherits a *stability theorem* recently proven for the fidelity correlator [44], which guarantees that a state with long-range order (LRO) in R_1 cannot be evolved to a state without such LRO by a strongly symmetric finite-depth channel.

Most importantly, the structural form of the Rényi-1 correlator naturally suggests a simple method with which SWSSB can be directly and scalably observed in a large class of mixed states. If the CP of ρ can be efficiently prepared, then measuring the Rényi-1 correlator trivially amounts to measuring a particular two-point correlation function. If this correlator exhibits LRO while ordinary

correlation functions of ρ do not, then one can immediately conclude that ρ exhibits SWSSB. Below we discuss several examples of CP states which can be prepared efficiently using standard techniques, and whose reduced density matrices naturally exhibit SWSSB.

Strong-To-Weak Spontaneous Symmetry Breaking.— A density matrix ρ of a quantum system is said to exhibit a strong symmetry under the group G if there is a unitary representation U_g of each $g \in G$ such that $U_g \rho = \rho U_g = e^{i\varphi_g} \rho$. In contrast, ρ is said to exhibit only a weak symmetry under G if $U_g \rho U_g^\dagger = \rho$. For concreteness, we will primarily consider the case of global on-site symmetries of many-body lattice spin models, where $U_g = \prod_j u_{j,g}$ factorizes across each local degree of freedom supported on the sites j of a regular lattice, although generalizations to higher-form symmetries have also been recently considered [29, 32, 34, 35]. Ordinary SSB in a state ρ with (at least) weak G -symmetry is then defined as LRO in the two-point correlation function $\text{tr}[O_x O_y^\dagger \rho]$ of a local operator O_x which is charged under the global symmetry, in the sense that $[O_x, U_g] \neq 0$ for some $g \in G$. In the mixed state setting, if ρ is strongly symmetric, it is said that such a state spontaneously breaks both the strong and weak symmetries.

Heuristically, a density matrix ρ exhibits SWSSB if its strong symmetry is spontaneously broken without breaking the corresponding weak symmetry. To make this notion precise, several recent works have defined SWSSB using the “Rényi-2” correlator $R_2(x, y)$ [17–19, 45], given by

$$R_2(x, y) := \frac{\text{tr}[O_x O_y^\dagger \rho O_x^\dagger O_y \rho]}{\text{tr} \rho^2} \quad (1)$$

$$= \frac{\langle\langle \rho | O_x^L \bar{O}_x^R [O_y^L \bar{O}_y^R]^\dagger | \rho \rangle\rangle}{\langle\langle \rho | \rho \rangle\rangle},$$

where in the second expression $|\rho\rangle\rangle := (\rho \otimes 1) \sum_s |s\rangle^L |s\rangle^R$ is the vectorization of ρ , with $\{|s\rangle^{L,R}\}$ denoting complete product-state bases of identical “left” and “right” subsystems L and R . The operators $O_x^L := O_x \otimes 1$ and $\bar{O}_x^R := 1 \otimes O_x^*$ respectively act only on the left and right subsystems. If ρ exhibits a strong symmetry under G , the doubled state $|\rho\rangle\rangle$ exhibits a doubled symmetry under the group $G^L \times G^R$: for any $g, h \in G$, $U_g^L \bar{U}_h^R |\rho\rangle\rangle = e^{i(\varphi_g - \varphi_h)} |\rho\rangle\rangle$. Using this formalism, SWSSB has been previously defined as LRO in the Rényi-2 correlator (1) in the absence of LRO in the ordinary two-point correlation function $\text{tr}[O_x O_y^\dagger \rho]$ [19, 45]. In the doubled-state representation, the order parameter $O_x^L \bar{O}_x^R$ transforms nontrivially under the separate symmetries G^L and G^R , but remains invariant [48] under the “diagonal” subgroup G^{diag} of $G^L \times G^R$ represented by $U_g^L \bar{U}_g^R$ for $g \in G$. For this reason, this definition of SWSSB can be interpreted in the doubled Hilbert space representation as the ordinary SSB of $G^L \times G^R$ down to a residual G^{diag} symmetry [19].

The Rényi-2 correlator is conceptually appealing and admits simple calculation methods in a variety of settings [17–19, 45]. Unfortunately, it suffers from two severe drawbacks. First, on the theoretical side, it has been recently observed that LRO in R_2 cannot be used to distinguish between different mixed-state phases [44]. That is, there exist simple examples of states within the same mixed-state phase—defined either by two-way connectivity via symmetric short-depth channels [35, 37, 39], or by more refined notions involving the non-divergence of the Markov length [40]—where one state exhibits long-range Rényi-2 correlations while the other does not. This behavior is closely related to the fact that R_2 is a second-moment observable in ρ ; by diagonalizing $\rho = \sum_i p_i |\psi_i\rangle\langle\psi_i|$ as an incoherent mixture of pure states, the states $|\psi_i\rangle$ are effectively sampled in Eq. (1) with the modified probabilities $p_i^2 / \sum_i p_i^2$, biasing the observable towards the most probable states in the mixture.

Second, R_2 is inherently difficult to observe in an experiment, even when the density matrix ρ is efficiently preparable. There exist several methods of measuring the purity $\text{tr} \rho^2$ in the denominator or the inner product $\text{tr}[\sigma \rho]$ of two density matrices in the numerator, such as the SWAP test [49] or classical shadow tomography [50–52]. However, since both of these quantities can be exponentially small in the system size for generic mixed states, the sample complexity of estimating these quantities with statistical error comparable to their means is exponentially large. Even worse, the ratio of these two exponentially small quantities will exhibit a scaled statistical error proportional to their inverse means. One therefore expects that *any* protocol for measuring R_2 will require exponentially many measurements.

A more robust theoretical measure of SWSSB is the fidelity correlator $F(x, y)$ proposed in Ref. [44], given by the fidelity between the density matrices ρ and $O_x O_y^\dagger \rho O_x^\dagger O_y$:

$$F(x, y) := \text{tr} \sqrt{\sqrt{\rho} O_x O_y^\dagger \rho O_x^\dagger O_y \sqrt{\rho}}. \quad (2)$$

The fidelity correlator has the appealing physical interpretation of diagnosing the *distinguishability* of ρ and $O_x O_y^\dagger \rho O_x^\dagger O_y$, offering a natural mixed-state generalization of charge condensation interpretations of SSB in pure states. Most importantly, the fidelity correlator admits a *stability theorem* [44]: if ρ exhibits SWSSB, in the sense that $F(x, y) \sim \mathcal{O}(1)$ as $|x - y| \rightarrow \infty$, and \mathcal{E} is a strongly symmetric finite-depth quantum channel, then $\mathcal{E}(\rho)$ also exhibits SWSSB. This means that any two states which are two-way connected by strongly symmetric finite-depth channels either both exhibit SWSSB or both do not exhibit SWSSB.

Unfortunately, the fidelity correlator is also inherently difficult to measure in experiment, with no obvious route towards measuring $F(x, y)$ beyond full-scale tomography. Additionally, the relation between LRO in $F(x, y)$ and

the spontaneous breaking of a strong symmetry is a priori unclear: as defined by the fidelity correlator, there is no *manifest* connection between SWSSB and ordinary SSB of a doubled symmetry group, as in the Rényi-2 definition.

Rényi-1 Correlator. — To alleviate these issues, we propose to define SWSSB using the “Rényi-1” correlator $R_1(x, y)$, which we define as

$$\begin{aligned} R_1(x, y) &:= \text{tr}[O_x O_y^\dagger \sqrt{\rho} O_x O_y^\dagger \sqrt{\rho}] \\ &= \langle\langle \sqrt{\rho} | O_x^L \bar{O}_x^R [O_y^L \bar{O}_y^R]^\dagger | \sqrt{\rho} \rangle\rangle, \end{aligned} \quad (3)$$

where $|\sqrt{\rho}\rangle\rangle := (\sqrt{\rho} \otimes 1) \sum_{\mathbf{s}} |\mathbf{s}\rangle^L |\mathbf{s}\rangle^R$ is the *canonical purification* (CP) of ρ [53], which has the useful property that $\text{tr}_R |\sqrt{\rho}\rangle\rangle \langle\langle \sqrt{\rho}| = \rho$. As with the vectorized state $|\rho\rangle\rangle$, a density matrix ρ with a strong G symmetry gives rise to a CP state $|\sqrt{\rho}\rangle\rangle$ with $G^L \times G^R$ symmetry, such that $U_g^L \bar{U}_h^R |\sqrt{\rho}\rangle\rangle = e^{i(\varphi_g - \varphi_h)} |\sqrt{\rho}\rangle\rangle$. Similar in spirit to the Rényi-2 correlator (1), the Rényi-1 correlator R_1 defines SWSSB in a strongly symmetric mixed state ρ as the conventional SSB of $G^L \times G^R$ symmetry in $|\sqrt{\rho}\rangle\rangle$ down to a residual G^{diag} symmetry.

Despite the aesthetic similarities to R_2 , R_1 also exhibits many close relations to the fidelity correlator (2) and the other information-theoretic observables for SWSSB proposed in Ref. [44]. In the Supplemental Material [53], we show that R_1 is *exactly* equal to the fidelity correlator for a large class of density matrices of recent theoretical interest: namely, stabilizer states affected by Pauli decoherence channels [17–19, 45], and thermal Gibbs states of stabilizer code Hamiltonians [54–57]. More generally, R_1 can be both upper and lower bounded by the fidelity correlator [53]:

$$[F(x, y)]^2 \leq R_1(x, y) \leq F(x, y), \quad (4)$$

where we have assumed for simplicity that $O_x O_y^\dagger$ is unitary, although this assumption can easily be relaxed. The latter inequality follows directly from Uhlmann’s theorem [58], while the former is a simple application of the Cauchy-Schwartz inequality. Thus, SWSSB as defined by LRO in R_1 and F are equivalent, and the former immediately inherits the stability theorem proven for the latter in Ref. [44].

In addition to the theoretical and aesthetic benefits of the Rényi-1 correlator mentioned above, the second line of Eq. (3) provides a direct method for potential experimental detection of SWSSB: if the CP state $|\sqrt{\rho}\rangle\rangle$ can be prepared efficiently, then $R_1(x, y)$ can easily be measured in this state as an ordinary two-point correlation function. LRO in $R_1(x, y)$ in the absence of LRO of $\text{tr}[O_x O_y^\dagger \rho] = \langle\langle \sqrt{\rho} | O_x^L [O_y^L]^\dagger | \sqrt{\rho} \rangle\rangle$ then immediately implies that the reduced density matrix on the “left” subsystem exhibits SWSSB.

Preparing Canonical Purifications. — We now provide several examples of CP states exhibiting SWSSB which

can be efficiently prepared in a quantum simulator. In order to demonstrate the techniques for constructing these states in the simplest setting, we focus here on simple examples of SWSSB in mixed states with strong \mathbb{Z}_2 symmetry.

Each of our examples consists of a system of N qubits with Pauli operators Z_j and X_j , arranged in a d -dimensional square lattice with periodic boundary conditions for concreteness. The initial state $\rho_0 = \prod_j |+\rangle\langle+|_j$ is a pure product state which is \mathbb{Z}_2 -symmetric under the parity operator $\Pi := \prod_j X_j$. Trivially, its CP $|\sqrt{\rho_0}\rangle\rangle = \prod_j (|+\rangle_j^L |+\rangle_j^R)$ is a pure product state on the doubled system LR , which is separately symmetric under the “left” parity $\Pi^L = \prod_j X_j^L$ and the “right” parity $\Pi^R = \prod_j X_j^R$. In the examples to follow, the CP $|\sqrt{\rho}\rangle\rangle$ of another density matrix ρ which exhibits SWSSB will spontaneously break these left and right parity symmetries, while remaining symmetric under the combined symmetry $\Pi^L \Pi^R$.

For our first example, we consider the effect of measuring $Z_i Z_j$ on each nearest-neighbor link $\langle ij \rangle$ of the lattice and discarding the measurement outcome; that is, we subject each nearest-neighbor link to the dephasing channel $\mathcal{E}_{ij}(\rho) = \frac{1}{2}(\rho + Z_i Z_j \rho Z_i Z_j)$. The resulting density matrix $\rho_\Pi := (1 + \Pi)/2^N$, which is an equally-weighted incoherent mixture of all parity-even states, is a paradigmatic example of a mixed state exhibiting \mathbb{Z}_2 SWSSB [31, 44]. Specifically, while $\text{tr}[Z_x Z_y \rho_\Pi] = 0$ for all $x \neq y$, all three of the observables (1), (2), and (3) are unity for $O_x = Z_x$ and $O_y = Z_y$.

It is easily verified that the canonical purification of ρ_Π is [53]

$$|\sqrt{\rho_\Pi}\rangle\rangle = 2^{(N-1)/2} \prod_{\langle ij \rangle} \left(\frac{1 + Z_i^L Z_i^R Z_j^L Z_j^R}{2} \right) |\sqrt{\rho_0}\rangle\rangle. \quad (5)$$

In other words, $|\sqrt{\rho_\Pi}\rangle\rangle$ is a stabilizer state with the $2N$ stabilizer generators $X_j^L X_j^R$, $Z_i^L Z_i^R Z_j^L Z_j^R$, and Π^L [59]. The easiest method of preparing the state (5) is to first prepare the state $|\text{GHZ}\rangle^L |+\rangle^R$, where $|\text{GHZ}\rangle \equiv \frac{1}{\sqrt{2}}(|0\rangle^{\otimes N} + |1\rangle^{\otimes N})$ is the N -qubit GHZ state and $|+\rangle \equiv \prod_j |+\rangle_j$, and then performing CNOT gates $CX_j^{R \rightarrow L} \equiv \frac{1}{2}(1 + X_j^L + Z_j^R - X_j^L Z_j^R)$ from each j th R qubit to the corresponding L qubit. The initial GHZ state can be prepared either in finite depth using $Z_i^L Z_j^L$ projective measurements and feedback [60–62], or in depth N via a sequential circuit of CNOT gates. Alternatively, one can directly prepare (5) via projective measurements of $Z_i^L Z_i^R Z_j^L Z_j^R$ and feedback, using an identical strategy as for the GHZ state.

The facility of preparing the CP state $|\sqrt{\rho_\Pi}\rangle\rangle$ was due to its stabilizer nature. Since the CP of any mixed stabilizer state is a pure stabilizer state [53], it is natural to seek a broader class of stabilizer mixed states featuring SWSSB. As our second example, we consider a simple

generalization of the preceding construction: rather than simply dephasing each link $\langle ij \rangle$, we *randomly* dephase each link with probability p . This results in a statistical ensemble of mixed states $\rho_\ell := [\prod_{\langle ij \rangle \in \ell} \mathcal{E}_{ij}](\rho_0)$ with corresponding probabilities $p_\ell = (1-p)^{dN-|\ell|}p^{|\ell|}$, where ℓ denotes the subset of dephased links and $|\ell|$ is the number of such links.

To understand the structure of the resulting states ρ_ℓ , consider first the effect of \mathcal{E}_{ij} on the initial state ρ_0 . Initially, the stabilizer group of ρ_0 is generated by $\{X_j\}_{j=1}^N$. Upon applying \mathcal{E}_{ij} , the individual stabilizers X_i and X_j are eliminated from the stabilizer group, but the stabilizer $X_i X_j$ remains. Thus, a new generating set is obtained by replacing X_i and X_j with their product $X_i X_j$. More generally, if ρ is a stabilizer state generated by a set of subregion parity operators $\Pi_{\mathcal{R}} := \prod_{j \in \mathcal{R}} X_j$, the channel \mathcal{E}_{ij} acting entirely within a region \mathcal{R} leaves ρ unaffected; conversely, if sites i and j belong to two distinct regions \mathcal{R} and \mathcal{R}' , then the individual generators $\Pi_{\mathcal{R}}$ and $\Pi_{\mathcal{R}'}$ are eliminated and replaced with their product $\Pi_{\mathcal{R} \cup \mathcal{R}'}$. Thus, each random sampling of dephased links ℓ yields a percolation configuration, i.e., a collection $\mathcal{P}(\ell)$ of connected clusters of sites \mathcal{R} , and ρ_ℓ is the stabilizer state generated by the subregion parities $\Pi_{\mathcal{R}}$ for each cluster $\mathcal{R} \in \mathcal{P}(\ell)$. In other words,

$$\rho_\ell = \frac{1}{2^N} \prod_{\mathcal{R} \in \mathcal{P}(\ell)} (1 + \Pi_{\mathcal{R}}). \quad (6)$$

It is easy to check that $\text{tr}[Z_x Z_y \rho_\ell] = 0$ for all $x \neq y$, but $R_1(x, y) = 1$ whenever x and y belong to the same region \mathcal{R} . Thus, the statistical ensemble of states ρ_ℓ undergoes a SWSSB transition for $d \geq 2$ in the universality class of d -dimensional bond percolation [63].

The CP states $|\sqrt{\rho_\ell}\rangle$ can be prepared in much the same way as Eq. (5): given a disorder realization ℓ , we simply apply the preceding protocol in each percolation cluster \mathcal{R} . Bond configurations ℓ can be easily sampled, and the number of clusters is at most of order N , so it is not substantially more difficult to prepare any given state $|\sqrt{\rho_\ell}\rangle$ than to prepare $|\sqrt{\rho_\Pi}\rangle$.

The general strategy of promoting a pure SSB state on the L subsystem to a CP state with SWSSB works for a large class of non-stabilizer states as well. For our third example, let $H := -\sum_{\langle ij \rangle} Z_i Z_j - g \sum_j X_j$ be the Hamiltonian of the transverse-field Ising model (TFIM) in d dimensions, and let $|\psi_g\rangle$ be its parity-even ground state as a function of the transverse field g . Notably, the wavefunction coefficients $\langle \{x\} | \psi_g \rangle$ of $|\psi_g\rangle$ in the X basis are positive for all $g \geq 0$ [64]. As a result, the state

$$\begin{aligned} |\Psi_g\rangle &:= \prod_j C X_j^{R \rightarrow L} |\psi_g\rangle^L |+\rangle^R \\ &= \sum_{\{x\}} \langle \{x\} | \psi_g \rangle |\{x\}\rangle^L |\{x\}\rangle^R \end{aligned} \quad (7)$$

is a valid CP state on LR . Moreover, it is easy to show that $\langle \langle \Psi_g | Z_x^L Z_y^L | \Psi_g \rangle \rangle$ vanishes for $x \neq y$, while

$$\langle \langle \Psi_g | Z_x^L Z_x^R Z_y^L Z_y^R | \Psi_g \rangle \rangle = \langle \psi_g | Z_x Z_y | \psi_g \rangle. \quad (8)$$

In other words, the reduced density matrix $\text{tr}_R |\Psi_g\rangle \langle \Psi_g|$ exhibits SWSSB in the ferromagnetic phase of H . More generally, any “sign-free” wavefunction on L , including the ground state of any “stoquastic” Hamiltonian [65], can be trivially converted to a CP state on LR by the same strategy. The reduced density matrices of the resulting states can then be used to construct a broad class of SWSSB states and transitions.

Since $|\psi_g\rangle$ is the ground state of a local gapped Hamiltonian, it can be efficiently prepared using adiabatic state preparation [66–69]. States in the paramagnetic phase are most easily achieved starting from the $g \rightarrow \infty$ ground state, while states in the ferromagnetic phase can be achieved by first constructing $|\psi_{g=0}\rangle = |\text{GHZ}\rangle$ and then adiabatically turning on g .

As a final example, we consider the thermal Gibbs state of the TFIM, with Hamiltonian H as above. Restricting to the parity-even sector via the projector $P_\Pi = \left(\frac{1+\Pi}{2}\right)$, the density matrix is $\rho_\beta := P_\Pi e^{-\beta H} / \text{tr}[P_\Pi e^{-\beta H}]$. The canonical purifications of thermal states are well-known as thermofield double (TFD) states [70–73]; in the present context, $|\sqrt{\rho_\beta}\rangle$ can be formally written using imaginary time evolution on $|\sqrt{\rho_\Pi}\rangle$:

$$|\sqrt{\rho_\beta}\rangle = \frac{1}{\sqrt{\text{tr}[P_\Pi e^{-\beta H}]}} \left(e^{-\beta H/2} \otimes 1 \right) |\sqrt{\rho_\Pi}\rangle. \quad (9)$$

At any finite temperature $\beta < \infty$ in $d = 1$, or above a critical temperature $\beta < \beta_c(g)$ in $d \geq 2$, the thermal density matrix ρ_β exhibits short-range ferromagnetic correlations: $\text{tr}[Z_x Z_y \rho_\beta] \rightarrow 0$ as $|x - y| \rightarrow \infty$. It has been previously argued that such a finite-temperature paramagnetic phase generically exhibits SWSSB [44]. This can be easily established in the extreme limits $g \rightarrow 0$ and $g \rightarrow \infty$, where the fidelity and Rényi-1 correlators are equal and can be computed exactly. In the Supplemental Material [53], we numerically demonstrate that the one-dimensional TFIM indeed exhibits SWSSB at all nonzero temperatures.

Here, rather than providing a specific algorithm for preparing $|\sqrt{\rho_\beta}\rangle$, we simply mention that several algorithms for preparing TFD states have already been proposed [74–77], and one of these has been experimentally tested in a trapped ion quantum computer [78]. These algorithms are largely based on variational approaches, in a similar spirit to the quantum approximate optimization algorithm [79]. A minor technical distinction between $|\sqrt{\rho_\beta}\rangle$ and the TFD states considered in these previous works is the restriction to the parity-even sector. As Eq. (9) shows, one simply needs to start their variational algorithm from the state $|\sqrt{\rho_\Pi}\rangle$ rather than a maximally entangled state on LR .

We end by mentioning a notable omission in this discussion: namely, the decohered quantum Ising model, a well-studied family of locally decohered states which exhibit a SWSSB transition [19, 44, 45]. These mixed states ρ_p are obtained from ρ_0 by applying the continuously tunable dephasing channel $\mathcal{E}_{ij}^p(\rho) = (1-p)\rho + pZ_iZ_j\rho Z_iZ_j$ to each nearest-neighbor link. In $d = 2$, ρ_p exhibits a SWSSB transition in the universality class of the random-bond Ising model on the Nishimori line, while in $d = 3$ there is a SWSSB transition in the universality class of the random-plaquette \mathbb{Z}_2 gauge theory on the Nishimori line. As reviewed in the Supplemental Material [53], the Rényi-1 and fidelity correlators can be directly related to disorder parameter correlations in these effective statistical physics models, *without* introducing additional replicas.

While it is trivial to construct a purification of ρ_p using a Stinespring dilation [58] of \mathcal{E}_{ij}^p , it is presently unclear how to transform this purification into the *canonical* purification. Such a transformation can be achieved by a deep unitary circuit on the ancillary qubits alone, but there is no obvious approach to explicitly construct or implement such a circuit. It is an interesting challenge for future work to find an explicit protocol for preparing the CPs of locally decohered mixed states such as ρ_p .

Discussion.— In this Letter, we have proposed the Rényi-1 correlator $R_1(x, y)$ as a diagnostic of SWSSB with several theoretically and practically useful properties. Similar to its Rényi-2 counterpart $R_2(x, y)$, $R_1(x, y)$ defines SWSSB in a mixed state ρ with G -symmetry as the spontaneous breaking of a doubled symmetry group $G^L \times G^R$ down to a diagonal subgroup G^{diag} . However, unlike R_2 , LRO in R_1 is robust under strongly symmetric finite-depth quantum channels due to the stability theorem it inherits from the fidelity correlator [44]. Moreover, the structure of R_1 as a two-point correlation function in the CP state $|\sqrt{\rho}\rangle$ suggests a simple protocol for observing SWSSB in experiments on quantum simulators: if such a CP state can be efficiently prepared, and it is shown to exhibit the aforementioned pattern of symmetry breaking, then its reduced density matrix necessarily exhibits SWSSB.

We have provided several simple examples of efficiently preparable CP states whose reduced density matrices exhibit SWSSB. For simplicity, we have restricted ourselves to CP states which are either stabilizer states (which are exceedingly simple to prepare) or to states which can be prepared using adiabatic evolution or other previously developed algorithms in the literature. It would be interesting to consider the design of bespoke quantum algorithms for the preparation of CP states, and in particular whether the CPs of mixed states arising from low-depth quantum channels are in general easy or difficult to prepare. Importantly, $|\sqrt{\rho}\rangle$ generally evolves *nonlinearly* as ρ evolves under such a channel, making it difficult to naively adapt previously developed state preparation

protocols to this setting.

Crucially, our method for observing SWSSB in a mixed state ρ requires access to a particular purification of ρ . Ideally, one would prefer a protocol for detecting SWSSB which only requires access to ρ itself. That is, given the ability to efficiently and repeatedly prepare an initially unknown mixed state ρ , one would like either a set of observables or perhaps a classical or quantum algorithm which can efficiently determine if ρ exhibits SWSSB. Since there are likely to exist many efficiently preparable mixed states whose CPs are not efficiently preparable, such a protocol would be a key step towards determining the practical physical implications of SWSSB in real quantum platforms.

Acknowledgements.— We thank Sajant Anand, Tyler Ellison, Tim Hsieh, Leonardo Lessa, Olumakinde Ogunnaike, Subhayan Sahu, Pablo Sala, and Chong Wang for insightful discussions, and especially Ehud Altman, Sam Garratt, and Zijian Wang for insightful discussions and helpful feedback on the manuscript. This material is based upon work supported by the U.S. Department of Energy, Office of Science, National Quantum Information Science Research Centers, Quantum Systems Accelerator.

Note added.— During the final stages of preparation of this manuscript, a preprint appeared [80] which also discusses the Rényi-1 correlator in the context of SWSSB. Our results agree where they overlap.

* zackmweinstein@berkeley.edu

- [1] S. Sachdev, *Quantum Phase Transitions* (Cambridge University Press, Cambridge, 2011).
- [2] S. Sachdev, *Quantum Phases of Matter* (Cambridge University Press, Cambridge, 2023).
- [3] E. Altman, K. R. Brown, G. Carleo, *et al.*, *PRX Quantum* **2**, 017003 (2021).
- [4] S. Ebadi, T. T. Wang, H. Levine, *et al.*, *Nature* **595**, 227 (2021).
- [5] K. J. Satzinger, Y.-J. Liu, A. Smith, *et al.*, *Science* **374**, 1237 (2021).
- [6] G. Semeghini, H. Levine, A. Keesling, *et al.*, *Science* **374**, 1242 (2021).
- [7] D. Bluvstein, H. Levine, G. Semeghini, *et al.*, *Nature* **604**, 451 (2022).
- [8] J. Léonard, S. Kim, J. Kwan, *et al.*, *Nature* **619**, 495 (2023).
- [9] E. H. Chen, G.-Y. Zhu, R. Verresen, *et al.*, *arXiv:2309.02863* (2023).
- [10] M. Iqbal, N. Tantivasadakarn, T. M. Gatterman, *et al.*, *Commun. Phys.* **7**, 1 (2024).
- [11] M. Iqbal, N. Tantivasadakarn, R. Verresen, *et al.*, *Nature* **626**, 505 (2024).
- [12] X. Mi, A. A. Michailidis, S. Shabani, *et al.*, *Science* **383**, 1332 (2024).
- [13] K. C. Miao, M. McEwen, J. Atalaya, *et al.*, *Nat. Phys.* **19**, 1780 (2023).

- [14] R. Acharya, L. Aghababaie-Beni, I. Aleiner, *et al.*, [arXiv:2408.13687 \(2024\)](#).
- [15] D. Bluvstein, S. J. Evered, A. A. Geim, *et al.*, *Nature* **626**, 58 (2024).
- [16] E. Dennis, A. Kitaev, A. Landahl, and J. Preskill, *J. Math. Phys.* **43**, 4452 (2002).
- [17] R. Fan, Y. Bao, E. Altman, and A. Vishwanath, *PRX Quantum* **5**, 020343 (2024).
- [18] Y. Bao, R. Fan, A. Vishwanath, and E. Altman, [arXiv:2301.05687 \(2023\)](#).
- [19] J. Y. Lee, C.-M. Jian, and C. Xu, *PRX Quantum* **4**, 030317 (2023).
- [20] Y. Zou, S. Sang, and T. H. Hsieh, *Phys. Rev. Lett.* **130**, 250403 (2023).
- [21] Y.-H. Chen and T. Grover, *Phys. Rev. Lett.* **132**, 170602 (2024).
- [22] K. Su, Z. Yang, and C.-M. Jian, *Phys. Rev. B* **110**, 085158 (2024).
- [23] Z. Li and R. S. K. Mong, [arXiv:2402.09516 \(2024\)](#).
- [24] T.-C. Lu, *Phys. Rev. B* **110**, 125145 (2024).
- [25] Y. Li, N. O'Dea, and V. Khemani, [arXiv:2406.15757 \(2024\)](#).
- [26] J. Hauser, Y. Bao, S. Sang, *et al.*, [arXiv:2407.07882 \(2024\)](#).
- [27] A. Sriram, N. O'Dea, Y. Li, *et al.*, [arXiv:2409.03325 \(2024\)](#).
- [28] P. Sala and R. Verresen, [arXiv:2409.12230 \(2024\)](#).
- [29] C. Zhang, Y. Xu, J.-H. Zhang, *et al.*, [arXiv:2409.17530 \(2024\)](#).
- [30] J. Y. Lee, Y.-Z. You, and C. Xu, [arXiv:2210.16323 \(2024\)](#).
- [31] R. Ma, J.-H. Zhang, Z. Bi, *et al.*, [arXiv:2305.16399 \(2024\)](#).
- [32] Z. Wang, Z. Wu, and Z. Wang, [arXiv:2307.13758 \(2024\)](#).
- [33] Y. Guo and Y. Ashida, *Phys. Rev. B* **109**, 195420 (2024).
- [34] R. Sohal and A. Prem, [arXiv:2403.13879 \(2024\)](#).
- [35] T. Ellison and M. Cheng, [arXiv:2405.02390 \(2024\)](#).
- [36] Z. Zhang, U. Agrawal, and S. Vijay, [arXiv:2405.05965 \(2024\)](#).
- [37] A. Coser and D. Pérez-García, *Quantum* **3**, 174 (2019).
- [38] T. Rakovszky, S. Gopalakrishnan, and C. von Keyserlingk, [arXiv:2308.15495 \(2024\)](#).
- [39] S. Sang, Y. Zou, and T. H. Hsieh, *Phys. Rev. X* **14**, 031044 (2024).
- [40] S. Sang and T. H. Hsieh, [arXiv:2404.07251 \(2024\)](#).
- [41] Y. Guo, K. Ding, and S. Yang, [arXiv:2408.03239 \(2024\)](#).
- [42] L. D. Landau, *Zh. Eksp. Teor. Fiz* **7**, 926 (1937).
- [43] J. McGreevy, *Annu. Rev. Condens. Matter Phys.* **14**, 57 (2023).
- [44] L. A. Lessa, R. Ma, J.-H. Zhang, *et al.*, [arXiv:2405.03639 \(2024\)](#).
- [45] P. Sala, S. Gopalakrishnan, M. Oshikawa, and Y. You, *Phys. Rev. B* **110**, 155150 (2024).
- [46] D. Gu, Z. Wang, and Z. Wang, [arXiv:2406.19381 \(2024\)](#).
- [47] X. Huang, M. Qi, J.-H. Zhang, and A. Lucas, [arXiv:2407.08760 \(2024\)](#).
- [48] In the case of a non-abelian symmetry, we have a multiplet of operators O_x^a which transform in a higher dimensional representation of G : $U_g^\dagger O_x^a U_g = \sum_b M_g^{ab} O_x^b$, where M_g^{ab} is a unitary matrix representation of $g \in G$. One should then replace $O_x^L \bar{O}_x^R$ with $\sum_a [O_x^a]^L [\bar{O}_x^a]^R$ to obtain an operator which transforms nontrivially under G^L and G^R but remains invariant under G^{diag} .
- [49] A. K. Ekert, C. M. Alves, D. K. L. Oi, *et al.*, *Phys. Rev. Lett.* **88**, 217901 (2002).
- [50] H.-Y. Huang, R. Kueng, and J. Preskill, *Nat. Phys.* **16**, 1050 (2020).
- [51] A. Elben, R. Kueng, H.-Y. R. Huang, *et al.*, *Phys. Rev. Lett.* **125**, 200501 (2020).
- [52] A. Elben, S. T. Flammia, H.-Y. Huang, *et al.*, *Nat. Rev. Phys.* **5**, 9 (2023).
- [53] See the Supplemental Material, which contains Refs. [81–90], for a review of canonical purification states, proofs of the upper and lower bounds on the Rényi-1 correlator, comparisons between the Rényi-1 correlator and other SWSSB observables in decohered stabilizer states and stabilizer Gibbs states, a replica-free calculation of the Rényi-1 and fidelity correlators in the decohered quantum Ising model, and a demonstration of SWSSB in the quantum Ising model at nonzero temperatures.
- [54] Z. Weinstein, G. Ortiz, and Z. Nussinov, *Phys. Rev. Lett.* **123**, 230503 (2019).
- [55] T.-C. Lu and T. Grover, *Phys. Rev. B* **99**, 075157 (2019).
- [56] T.-C. Lu, T. H. Hsieh, and T. Grover, *Phys. Rev. Lett.* **125**, 116801 (2020).
- [57] Y. Li, C. W. von Keyserlingk, G. Zhu, and T. Jochym-O'Connor, *Phys. Rev. Res.* **6**, 043007 (2024).
- [58] M. A. Nielsen and I. L. Chuang, *Quantum Computation and Quantum Information* (Cambridge University Press, 2010).
- [59] Note that Π^R is also a stabilizer, obtained from the product of generators $\Pi^L \prod_j X_j^L X_j^R$.
- [60] N. Tantivasadakarn, R. Thorngren, A. Vishwanath, and R. Verresen, *Phys. Rev. X* **14**, 021040 (2024).
- [61] J. Y. Lee, W. Ji, Z. Bi, and M. P. A. Fisher, [arXiv:2208.11699 \(2022\)](#).
- [62] G.-Y. Zhu, N. Tantivasadakarn, A. Vishwanath, *et al.*, *Phys. Rev. Lett.* **131**, 200201 (2023).
- [63] D. Stauffer and A. Aharony, *Introduction To Percolation Theory* (Taylor & Francis, 2018).
- [64] A. Auerbach, *Interacting Electrons and Quantum Magnetism*, Graduate Texts in Contemporary Physics (Springer New York, New York, NY, 1994).
- [65] S. Bravyi, D. P. Divincenzo, R. Oliveira, and B. M. Terhal, *Quantum Info. Comput.* **8**, 361 (2008).
- [66] E. Farhi, J. Goldstone, S. Gutmann, and M. Sipser, [arXiv:quant-ph/0001106 \(2000\)](#).
- [67] A. Das and B. K. Chakrabarti, *Rev. Mod. Phys.* **80**, 1061 (2008).
- [68] I. M. Georgescu, S. Ashhab, and F. Nori, *Rev. Mod. Phys.* **86**, 153 (2014).
- [69] T. Albash and D. A. Lidar, *Rev. Mod. Phys.* **90**, 015002 (2018).
- [70] Y. Takahashi and H. Umezawa, *Int. J. Mod. Phys. B* **10**, 1755 (1996).
- [71] J. Maldacena, *J. High Energy Phys.* **2003** (04), 021.
- [72] J. Maldacena and L. Susskind, *Fortschr. Phys.* **61**, 781 (2013).
- [73] J. Maldacena and X.-L. Qi, [arXiv:1804.00491 \(2018\)](#).
- [74] J. Wu and T. H. Hsieh, *Phys. Rev. Lett.* **123**, 220502 (2019).
- [75] W. Cottrell, B. Freivogel, D. M. Hofman, and S. F. Lokhande, *J. High Energy Phys.* **2019** (2), 58.
- [76] J. Martyn and B. Swingle, *Phys. Rev. A* **100**, 032107 (2019).
- [77] V. P. Su, *Phys. Rev. A* **104**, 012427 (2021).

- [78] D. Zhu, S. Johri, N. M. Linke, *et al.*, *Proc. Natl. Acad. Sci.* **117**, 25402 (2020).
- [79] E. Farhi, J. Goldstone, and S. Gutmann, *arXiv:1411.4028* (2014).
- [80] Z. Liu, L. Chen, Y. Zhang, *et al.*, *arXiv:2410.09327* (2024).
- [81] S. Aaronson and D. Gottesman, *Phys. Rev. A* **70**, 052328 (2004).
- [82] S. Paeckel, T. Köhler, A. Swoboda, *et al.*, *Ann. Phys.* **411**, 167998 (2019).
- [83] F. J. Wegner, *J. Math. Phys.* **12**, 2259 (1971).
- [84] C. Wang, J. Harrington, and J. Preskill, *Ann. Phys.* **303**, 31 (2003).
- [85] A. Honecker, M. Picco, and P. Pujol, *Phys. Rev. Lett.* **87**, 047201 (2001).
- [86] T. Ohno, G. Arakawa, I. Ichinose, and T. Matsui, *Nucl. Phys. B* **697**, 462 (2004).
- [87] A. L. Talapov and H. W. J. Blöte, *J. Phys. A* **29**, 5727 (1996).
- [88] Z. Weinstein, R. Sajith, E. Altman, and S. J. Garratt, *Phys. Rev. B* **107**, 245132 (2023).
- [89] L. G. Molinari, *arXiv:1710.09248* (2023).
- [90] M. Wimmer, *ACM Trans. Math. Softw.* **38**, 1 (2012).

Supplemental Material For: Efficient Detection of Strong-To-Weak Spontaneous Symmetry Breaking via the Rényi-1 Correlator

Zack Weinstein

Department of Physics, University of California, Berkeley, CA 94720, USA

(Dated: November 1, 2024)

CONTENTS

Acknowledgments	5
References	5
SI. Canonical Purification States	8
A. Thermofield Double States	9
B. Canonical Purifications of Stabilizer States	9
SII. Upper and Lower Bounds on the Rényi-1 Correlator	10
SIII. Comparison of Rényi-1 Correlator and Other Measures of SWSSB	11
A. Stabilizer States under Pauli Noise	12
B. Gibbs States of Stabilizer Code Hamiltonians	13
SIV. Strong-To-Weak Spontaneous Symmetry-Breaking in the Decohered Quantum Ising Model	14
A. High-Temperature Expansion	16
B. Low-Temperature Expansion	17
$d = 2$: Random-Bond Ising Model on the Nishimori Line	17
$d = 3$: Random-Plaquette \mathbb{Z}_2 Gauge Theory	19
C. Rényi-2 Correlations and Annealed Averages	20
SV. Strong-To-Weak Spontaneous Symmetry Breaking in the One-Dimensional Transverse-Field Ising Model at Nonzero Temperatures	20

SI. CANONICAL PURIFICATION STATES

In this Appendix, we provide a brief overview of canonical purification (CP) states. After explaining general features of these states, we specialize to describing the CPs of two particular cases of physical interest: namely, stabilizer mixed states, and Gibbs states.

Let $\rho = \sum_i p_i |\psi_i\rangle\langle\psi_i|$ be a density matrix of a quantum system, written without loss of generality as an incoherent mixture of orthonormal pure states $|\psi_i\rangle$. As its name suggests, the CP of ρ is a particular purification of ρ , obtained as follows. First, since ρ is nonnegative, its square root $\sqrt{\rho} = \sum_i \sqrt{p_i} |\psi_i\rangle\langle\psi_i|$ is a well-defined nonnegative Hermitian operator. Then, labeling the original system as L and introducing an identical copy of the system labeled R (‘left’ and ‘right’ respectively), we obtain the CP state $|\sqrt{\rho}\rangle\rangle$ by acting $\sqrt{\rho}$ on the left half of an (unnormalized) maximally entangled state:

$$|\sqrt{\rho}\rangle\rangle := (\sqrt{\rho} \otimes 1) \sum_{\mathbf{s}} |\mathbf{s}\rangle^L |\mathbf{s}\rangle^R = \sum_i \sqrt{p_i} |\psi_i\rangle^L |\psi_i^*\rangle^R, \quad (\text{S1})$$

where $|\mathbf{s}\rangle$ is a complete orthonormal basis of the original system, and the state $|\psi_i^*\rangle$ has complex-conjugated matrix elements $\langle \mathbf{s} | \psi_i^* \rangle = \langle \mathbf{s} | \psi_i \rangle^*$ relative to $|\psi_i\rangle$. We use kets with doubled angular brackets $|\cdot\rangle\rangle$ to denote states in the doubled Hilbert space LR , kets with single brackets and a superscript $|\cdot\rangle^{L,R}$ to denote states in the left or right Hilbert space, and single brackets without a superscript $|\cdot\rangle$ to denote states in the original Hilbert space.

Despite its name, the canonical purification $|\sqrt{\rho}\rangle\rangle$ is not entirely unique; it requires a particular choice of basis $|\mathbf{s}\rangle$ of the original Hilbert space, and different choices of basis need not yield the same state $|\sqrt{\rho}\rangle\rangle$. In particular, the complex conjugation operation required to obtain $|\psi_i^*\rangle$ from $|\psi_i\rangle$ is basis-dependent: complex conjugation of

wavefunction coefficients in two different bases need not agree. The canonical purifications constructed with two different sets of bases $|\mathbf{r}\rangle$ and $|\mathbf{s}\rangle$ agree if they are related by an *orthogonal* transformation, i.e., $|\mathbf{r}\rangle = \sum_{\mathbf{s}} \mathbf{O}_{\mathbf{rs}} |\mathbf{s}\rangle$ with $\sum_{\mathbf{r}} \mathbf{O}_{\mathbf{rs}} \mathbf{O}_{\mathbf{rs}'} = \delta_{\mathbf{ss}'}$. For example, in a system of qubits, canonical purifications defined with respect to the Pauli-Z eigenbasis and the Pauli-X eigenbasis are equivalent. Throughout this work, we assume that the basis $|\mathbf{s}\rangle$ is the computational basis, i.e., the Pauli-Z eigenbasis.

Any two purifications of a quantum mixed state are equivalent up to an isometry V on the auxiliary system; this follows easily from the uniqueness properties of the Schmidt decomposition [58]. In other words, an arbitrary purification $|\Psi_\rho\rangle\rangle$ of ρ can be written as

$$|\Psi_\rho\rangle\rangle^{LA} = (1 \otimes V^{A \leftarrow R}) |\sqrt{\rho}\rangle\rangle = (\sqrt{\rho} \otimes V^{A \leftarrow R}) \sum_{\mathbf{s}} |\mathbf{s}\rangle^L |\mathbf{s}\rangle^R. \quad (\text{S2})$$

Thus, *any* purification of ρ can be brought to the form of a canonical purification by an isometry acting on the auxiliary space A alone. Note that the dimension of the auxiliary Hilbert space A must be at least as large as the rank of ρ . Therefore, for a generic density matrix of full rank, the auxiliary system A must be at least as large as R .

Naturally, since $|\sqrt{\rho}\rangle\rangle$ is a purification of ρ , expectation values of observables $O^L := (O \otimes 1)$ in the left subsystem alone reproduce expectation values of ρ : $\langle\langle \sqrt{\rho} | O^L | \sqrt{\rho} \rangle\rangle = \text{tr}[O\rho]$. Meanwhile, expectation values of observables $\bar{O}^R := (1 \otimes O^*)$ yield $\langle\langle \sqrt{\rho} | \bar{O}^R | \sqrt{\rho} \rangle\rangle = \text{tr}[\rho O^\dagger]$. Finally, general two-sided expectation values can be written in terms of a trace as $\langle\langle \sqrt{\rho} | O_1^L \bar{O}_2^R | \sqrt{\rho} \rangle\rangle = \text{tr}[O_1 \sqrt{\rho} O_2^\dagger \sqrt{\rho}]$. Each of these identities can be derived by simple index-chasing, or more rapidly via tensor network diagrams.

We now discuss two broad classes of canonical purification states with insightful formal expressions.

A. Thermofield Double States

First, we consider the case of a thermal state $\rho_\beta := e^{-\beta H} / \mathcal{Z}_\beta$, where $\mathcal{Z}_\beta := \text{tr} e^{-\beta H}$ is the partition function of the Hamiltonian H at inverse temperature β . In this setting, the canonical purification of ρ_β is referred to as the thermofield double (TFD) state. It is frequently written in the following various forms:

$$\begin{aligned} |\sqrt{\rho_\beta}\rangle\rangle &= \frac{1}{\sqrt{\mathcal{Z}_\beta}} \left(e^{-\beta H/2} \otimes 1 \right) \sum_{\mathbf{s}} |\mathbf{s}\rangle^L |\mathbf{s}\rangle^R \\ &= \frac{1}{\sqrt{\mathcal{Z}_\beta}} \left(e^{-\beta H/4} \otimes e^{-\beta H^T/4} \right) \sum_{\mathbf{s}} |\mathbf{s}\rangle^L |\mathbf{s}\rangle^R \\ &= \frac{1}{\sqrt{\mathcal{Z}_\beta}} \sum_n e^{-\beta E_n/2} |E_n\rangle^L |E_n^*\rangle^R, \end{aligned} \quad (\text{S3})$$

where $|E_n\rangle$ are the energy eigenstates of H with the energies E_n . In the middle expression, we have split up the factor of $e^{-\beta H/2}$ across the two copies L and R of the system, which requires replacing H with H^T in the right subsystem. Since H is Hermitian, we could equivalently write $H^* = H^T$, where H^* is the matrix with complex conjugated matrix elements in the basis $|\mathbf{s}\rangle$. Note that two-sided correlation functions, such as the Rényi-1 correlator [Eq. (S9)], have a particularly simple interpretation in the TFD state $|\sqrt{\rho_\beta}\rangle\rangle$: they are simply imaginary time-ordered correlation functions, with one operator evolved to imaginary time $\tau = \beta/2$:

$$\begin{aligned} \langle\langle \sqrt{\rho_\beta} | O_1^L \bar{O}_2^R | \sqrt{\rho_\beta} \rangle\rangle &= \frac{1}{\mathcal{Z}_\beta} \text{tr} \left[e^{-\beta H/2} O_1 e^{-\beta H/2} O_2^\dagger \right] \\ &= \frac{1}{\mathcal{Z}_\beta} \text{tr} \left[e^{-\beta H} \left(e^{\beta H/2} O_1 e^{-\beta H/2} \right) O_2^\dagger \right] \\ &= \left\langle O_1(\tau = \beta/2) O_2^\dagger(\tau = 0) \right\rangle_\beta. \end{aligned} \quad (\text{S4})$$

B. Canonical Purifications of Stabilizer States

Second, we consider the case of a stabilizer state $\rho_{\mathcal{S}}$. Let \mathcal{S} be an $[[N, k]]$ stabilizer code on N physical qubits with $N - k$ generators g_1, \dots, g_{N-k} , and $2k$ logical operators $\mathcal{Z}_n, \mathcal{X}_n$. All of the generators commute amongst each other

and with all of the logical operators, while the logical operators form a Pauli algebra of k qubits:

$$[g_a, g_b] = 0, \quad [g_a, \mathcal{Z}_n] = [g_a, \mathcal{X}_n] = 0, \quad [\mathcal{Z}_n, \mathcal{Z}_m] = [\mathcal{X}_n, \mathcal{X}_m] = 0, \quad \{\mathcal{Z}_n, \mathcal{X}_m\} = \delta_{nm}. \quad (\text{S5})$$

The stabilizer state $\rho_{\mathcal{S}}$ is defined as the uniform projector onto the 2^k -dimensional stabilizer subspace $V_{\mathcal{S}} = \{|\psi\rangle : g|\psi\rangle = |\psi\rangle, g \in \mathcal{S}\}$. It can be written explicitly in terms of the generators g_a as

$$\rho_{\mathcal{S}} = \frac{1}{2^k} \prod_{a=1}^{N-k} \left(\frac{1 + g_a}{2} \right). \quad (\text{S6})$$

In this form, it is trivial to take the square root: $\sqrt{\rho_{\mathcal{S}}} = 2^{k/2} \rho_{\mathcal{S}}$. To obtain $|\sqrt{\rho_{\mathcal{S}}}\rangle$, we simply act $\sqrt{\rho_{\mathcal{S}}}$ on the left side of the maximally entangled state, $|\Phi\rangle \propto \sum_{\mathbf{s}} |\mathbf{s}\rangle^L |\mathbf{s}\rangle^R$. This state is itself a stabilizer state, with a stabilizer group generated by $X_j^L X_j^R$ and $Z_j^L Z_j^R$ for $j = 1, \dots, N$. The projectors $\frac{1}{2}(1 + g_a^L)$ can then be understood as projective measurements of the stabilizers g_a^L performed on the left system, with the postselected outcomes $+1$; this reorganizes the stabilizer group by eliminating all stabilizers which anticommute with g_a^L and appending these generators to the generating set. To determine the resulting stabilizer group, it is convenient to first perform a change of basis on the generators of $|\Phi\rangle$. By inspection, we can choose to represent the stabilizer group $\mathcal{S}(|\Phi\rangle)$ of $|\Phi\rangle$ with the following set of generators:

$$\mathcal{S}(|\Phi\rangle) = \langle g_a^L \bar{g}_a^R, \quad h_a^L \bar{h}_a^R, \quad \mathcal{Z}_n^L \bar{\mathcal{Z}}_n^R, \quad \mathcal{X}_n^L \bar{\mathcal{X}}_n^R \rangle, \quad (\text{S7})$$

where the h_a operators are the ‘destabilizers’ [81], i.e., Pauli operators which satisfy $\{g_a, h_b\} = \delta_{ab}$ and complete the algebra $\{g_a, \mathcal{Z}_n, \mathcal{X}_n\}$ into a full N -qubit Pauli algebra. After measuring each g_a^L , the generators $h_a^L \bar{h}_a^R$ are eliminated, and we have the following stabilizer group¹ for $|\sqrt{\rho_{\mathcal{S}}}\rangle$:

$$\mathcal{S}(|\sqrt{\rho_{\mathcal{S}}}\rangle) = \langle g_a^L, \quad \bar{g}_a^R, \quad \mathcal{Z}_n^L \bar{\mathcal{Z}}_n^R, \quad \mathcal{X}_n^L \bar{\mathcal{X}}_n^R \rangle. \quad (\text{S8})$$

This prescription gives an easy recipe for constructing the canonical purification of any stabilizer state $\rho_{\mathcal{S}}$: introduce two copies of the system, one in the state $\rho_{\mathcal{S}}$ and the other in the state $\rho_{\mathcal{S}}^*$, and then maximally entangle their logical spaces by introducing the $2k$ additional stabilizers $\mathcal{Z}_n^L \bar{\mathcal{Z}}_n^R, \mathcal{X}_n^L \bar{\mathcal{X}}_n^R$.

SII. UPPER AND LOWER BOUNDS ON THE RÉNYI-1 CORRELATOR

In this Appendix, we show that the Rényi-1 correlator $R_1(x, y)$ of an operator O_x , defined by

$$R_1(x, y) := \text{tr} [O_x O_y^\dagger \sqrt{\rho} O_y O_x^\dagger \sqrt{\rho}] = \langle\langle \sqrt{\rho} | O_x^L \bar{O}_x^R [O_y^L \bar{O}_y^R]^\dagger | \sqrt{\rho} \rangle\rangle, \quad (\text{S9})$$

can be upper and lower bounded by the fidelity correlator $F(x, y)$ of the same operator, defined by

$$F(x, y) := \text{tr} \sqrt{\sqrt{\rho} O_x O_y^\dagger \rho O_y O_x^\dagger \sqrt{\rho}}. \quad (\text{S10})$$

Ref. [44] proposed to define strong-to-weak spontaneous symmetry breaking (SWSSB) via long-range order (LRO) in the fidelity correlator $F(x, y)$ in the absence of LRO in ordinary correlators $\text{tr} [O_x O_y^\dagger \rho]$. The inequalities derived below [Eq. (S14)] imply that long-range order in $F(x, y)$ and the Rényi-1 correlator $R_1(x, y)$ are equivalent, and can be used interchangeably to define SWSSB. Consequently, the Rényi-1 correlator immediately inherits the stability theorem proven for the fidelity correlator in Ref. [44]: if ρ exhibits LRO in $R_1(x, y)$ [i.e., $R_1(x, y) \sim \mathcal{O}(1)$ as $|x - y| \rightarrow \infty$], and \mathcal{E} is a strongly symmetric finite-depth quantum channel, then $\mathcal{E}(\rho)$ also exhibits LRO² in $R_1(x, y)$.

For convenience of notation, let $\sigma \equiv O_x O_y^\dagger \rho O_y O_x^\dagger$. We assume for simplicity that $O_x O_y^\dagger$ is unitary (such as when O_x and O_y are Pauli operators) so that σ is a valid density matrix, although this assumption can easily be relaxed.

¹ To make contact with the expression for $|\sqrt{\rho_{\Pi}}\rangle$ provided in the main text, we use the single generator Π for our stabilizer group, the single destabilizer Z_1 , and the $2(N-1)$ logical operators X_2, \dots, X_N and $Z_1 Z_2, \dots, Z_1 Z_N$. After the postselected measurement, the stabilizer group of the doubled state is generated by $\Pi^L, \Pi^R, X_j^L X_j^R$, and $Z_1^L Z_1^R Z_j^L Z_j^R$ for $j = 2, \dots, N$.

² A minor subtlety is that, in general, the charged operator O_x used in R_1 before the channel is applied may be different than the charged operator used in R_1 after the channel is applied.

The upper bound on R_1 follows trivially from Uhlmann's theorem [58], which states that the fidelity between two density matrices σ and ρ is given by the supremum of all pure-state overlaps $\langle\langle \Psi_\sigma | \Phi_\rho \rangle\rangle$, where $|\Psi_\sigma\rangle\rangle$ and $|\Phi_\rho\rangle\rangle$ are purifications of ρ and σ respectively. Using the above definition of σ , R_1 can be written as

$$R_1(x, y) = \text{tr}[\sqrt{\sigma}\sqrt{\rho}] = \langle\langle \sqrt{\sigma} | \sqrt{\rho} \rangle\rangle \leq \max_{|\Psi_\sigma\rangle\rangle, |\Phi_\rho\rangle\rangle} \langle\langle \Psi_\sigma | \Phi_\rho \rangle\rangle = F(x, y). \quad (\text{S11})$$

In words, since $|\sigma\rangle\rangle$ and $|\rho\rangle\rangle$ are themselves purifications of σ and ρ , their overlap is necessarily no larger than the fidelity between the two states.

To achieve a lower bound, note first that $\sqrt{\sigma}\sqrt{\rho}$ can be written via polar decomposition as $U\sqrt{\sqrt{\rho}\sigma\sqrt{\rho}}$ for some unitary U . This allows for the fidelity to be written as

$$\begin{aligned} F(x, y) &= \text{tr}[U^\dagger \sqrt{\sigma}\sqrt{\rho}] = \text{tr}\left[(\sigma^{1/4}U\rho^{1/4})^\dagger(\sigma^{1/4}\rho^{1/4})\right] \\ &\leq \sqrt{\text{tr}[(\sigma^{1/4}U\rho^{1/4})^\dagger(\sigma^{1/4}U\rho^{1/4})] \text{tr}[(\sigma^{1/4}\rho^{1/4})^\dagger(\sigma^{1/4}\rho^{1/4})]}, \end{aligned} \quad (\text{S12})$$

where we have used the cyclicity of the trace and the Cauchy-Schwartz inequality for the Hilbert-Schmidt inner product, $\text{tr}[A^\dagger B] \leq \sqrt{\text{tr}[A^\dagger A] \text{tr}[B^\dagger B]}$. The second term inside the square root is simply R_1 , while the first term can be upper-bounded using the Cauchy-Schwartz inequality once again:

$$\text{tr}[(\sigma^{1/4}U\rho^{1/4})^\dagger(\sigma^{1/4}U\rho^{1/4})] = \text{tr}[\sqrt{\rho}U^\dagger\sqrt{\sigma}U] \leq \sqrt{\text{tr}[\rho] \text{tr}[U^\dagger\sigma U]} = 1. \quad (\text{S13})$$

We thus arrive at the inequality $F(x, y) \leq \sqrt{R_1(x, y)}$. Altogether, we obtain the following upper and lower bounds on the Rényi-1 correlator:

$$[F(x, y)]^2 \leq R_1(x, y) \leq F(x, y), \quad (\text{S14})$$

valid whenever $O_x O_y^\dagger$ is unitary. As a sanity check, note that $0 \leq F(x, y) \leq 1$ and $0 \leq R_1(x, y) \leq 1$, as follows directly from their definitions.

SIII. COMPARISON OF RÉNYI-1 CORRELATOR AND OTHER MEASURES OF SWSSB

In this Appendix, we show that the Rényi-1 correlator of a charged operator O_x , defined by Eq. (S9), is easily computable for two broad physical settings of theoretical interest: namely, stabilizer states under Pauli noise, and thermal Gibbs states of stabilizer code Hamiltonians. In both cases, it is exactly equal to the recently proposed fidelity correlator of Eq. (S10). For simplicity, we shall assume throughout that O_x is a Pauli operator, so that $O \equiv O_x O_y^\dagger$ is unitary and $O\rho O^\dagger$ is a valid density matrix.

Along the way, we shall compare $R_1(x, y)$ with several other recently proposed diagnostics of strong-to-weak spontaneous symmetry breaking (SWSSB): namely, the fidelity correlator (S10), relative entropy correlator,

$$\mathcal{D}(x, y) := \text{tr}\left\{\rho[\log \rho - \log(O_x O_y^\dagger \rho O_y O_x^\dagger)]\right\}, \quad (\text{S15})$$

the trace distance correlator,

$$D_1(x, y) := \frac{1}{2} \|\rho - O_x O_y^\dagger \rho O_y O_x^\dagger\|_1, \quad (\text{S16})$$

and the Rényi-2 correlator,

$$R_2(x, y) := \frac{\text{tr}[O_x O_y^\dagger \rho O_y O_x^\dagger]}{\text{tr} \rho^2} = \frac{\langle\langle \rho | O_x^L \bar{O}_x^R [O_y^L \bar{O}_y^R]^\dagger | \rho \rangle\rangle}{\langle\langle \rho | \rho \rangle\rangle}. \quad (\text{S17})$$

Eqs. (S10), (S15), and (S16), proposed by Refs. [17–19, 44], exhibit operationally meaningful information-theoretic interpretations, and the fidelity correlator in particular admits a useful “stability theorem” [44]. The Rényi-2 correlator, which has received the most direct attention thus far [17–19, 29, 45], offers a particularly transparent interpretation of SWSSB in terms of spontaneously breaking “left” and “right” symmetries of a doubled system down to a diagonal subgroup; however, as we shall see below, it generically disagrees with the previously mentioned observables on whether

a given mixed state exhibits SWSSB, and is expected to exhibit critical phenomena in an altogether different universality class. In particular, R_2 does not respect two-way connectivity, in the sense that a state with long-range Rényi-2 correlations and a state without such correlations can be two-way connected by finite-depth symmetric channels.

In contrast to all of these observables, the Rényi-1 correlator combines the best features of both the Rényi-2 correlator and the fidelity correlator: it admits similar symmetry-breaking interpretations to the Rényi-2 correlator, and it inherits the stability theorem from the fidelity correlator due to the two-sided bound proven in Appendix [SII](#).

A. Stabilizer States under Pauli Noise

Let $\mathcal{S} = \langle g_1, \dots, g_{N-k} \rangle$ be an $[[N, k]]$ stabilizer code on N physical qubits as defined in Appendix [SI](#). We initialize our N -qubit system in the stabilizer state $\rho_{\mathcal{S}}$ of \mathcal{S} , as in Eq. [\(S6\)](#). The system is then subjected to a general Pauli channel \mathcal{E} , which applies the Pauli error e with probability p_e :

$$\rho = \mathcal{E}(\rho_{\mathcal{S}}) = \sum_{e \in \mathcal{P}_N} p_e e \rho_{\mathcal{S}} e^\dagger, \quad \sum_{e \in \mathcal{P}_N} p_e = 1, \quad (\text{S18})$$

where \mathcal{P}_N is the group of N -qubit Pauli strings, together with phases $\pm 1, \pm i$. Note that each Pauli error $e \in \mathcal{P}_N$ is unitary, so that \mathcal{E} is a proper quantum channel.

The number of distinct Pauli errors $e \in \mathcal{P}_N$ is exponentially large in N . Many of these errors act *degenerately* on the state $\rho_{\mathcal{S}}$; two errors e and e' are called degenerate, and are grouped into the same equivalence class $s = [e]$, if $e \rho_{\mathcal{S}} e^\dagger = e' \rho_{\mathcal{S}} e'^\dagger$. If \mathcal{S} is regarded as a quantum error correcting code encoding k logical qubits, then each equivalence class s is a set of errors which yield the same syndrome measurement. We can partially simplify the state ρ by writing it as a sum over a smaller (but still exponentially large) set of equivalence classes s :

$$\rho = \sum_s P_s \rho_s, \quad P_s = \sum_{e \in s} p_e, \quad \rho_s = e \rho_{\mathcal{S}} e^\dagger \text{ for } e \in s. \quad (\text{S19})$$

Crucially, the density matrices ρ_s corresponding to particular syndrome measurements are orthogonal projectors, such that $\rho_s \rho_{s'} = \frac{1}{2^k} \delta_{ss'} \rho_s$. This follows from the original definition [\(S6\)](#) of $\rho_{\mathcal{S}}$ as a projector onto a stabilizer space, and the observation that a given Pauli error e can only commute or anticommute with the generators g_a . As a result, each state $e \rho_{\mathcal{S}} e^\dagger$ is itself a projector onto a stabilizer space, where we obtain the new stabilizer group by simply flipping the sign of each generator which anticommutes with e .

The above representation of ρ remains purely formal. Nevertheless, many information-theoretic observables can be usefully expressed in this formal representation. For example, if O is a general Pauli operator and Os denotes the left coset³ of the equivalence class s by O , then

$$O \rho O^\dagger = \sum_s P_s O \rho_s O^\dagger = \sum_s P_s \rho_{Os} = \sum_s P_{Os} \rho_s. \quad (\text{S20})$$

Additionally, the square root $\sqrt{\rho}$ and logarithm $\log \rho$ of ρ can easily be computed, giving the results⁴

$$\sqrt{\rho} = 2^{k/2} \sum_s \sqrt{P_s} \rho_s, \quad \log \rho = -k + 2^k \sum_s [\log P_s] \rho_s. \quad (\text{S21})$$

Using these, we can immediately obtain formal expressions for a variety of information-theoretic probes of SWSSB. Letting $O \equiv O_x O_y^\dagger$ in Eq. [\(S9\)](#), the Rényi-1 correlator is immediately given by

$$R_1(x, y) = \sum_s \sqrt{P_{Os} P_s} = \sum_s P_s \sqrt{\frac{P_{Os}}{P_s}} = \sum_{e \in \mathcal{P}_N} p_e \sqrt{\frac{P_{[Oe]}}{P_{[e]}}}, \quad (\text{S22})$$

³ In other words, if e is a representative of the equivalence class s (i.e., $s = [e]$), then $Os := [Oe]$.

⁴ Strictly speaking, the logarithm is not well-defined if $P_s = 0$ for some s (equivalently, if the set of projectors ρ_s with nonzero weight in ρ do not form a complete set). In computing $\mathcal{D}(x, y)$, we set $P_s \log P_{s'} = 0$ if $P_s = P_{s'} = 0$, and $P_s \log P_{s'} = -\infty$ if $P_{s'} = 0 \neq P_s$.

where we have used the fact that $P_{[e]}$ depends only on the equivalence class e to write R_1 as a sum over all Pauli errors. Similarly, the correlators of Eqs. (S10), (S15), (S16), (S17) can be formally written as

$$F(x, y) = \sum_s \sqrt{P_{Os} P_s} = \sum_{e \in \mathcal{P}_N} p_e \sqrt{\frac{P_{[Oe]}}{P_{[e]}}}, \quad (\text{S23a})$$

$$\mathcal{D}(x, y) = - \sum_s P_s \log \left\{ \frac{P_{Os}}{P_s} \right\} = - \sum_{e \in \mathcal{P}_N} p_e \log \left\{ \frac{P_{[Oe]}}{P_{[e]}} \right\}, \quad (\text{S23b})$$

$$D_1(x, y) = \frac{1}{2} \sum_s |P_s - P_{Os}| = \frac{1}{2} \sum_{e \in \mathcal{P}_N} p_e \left| 1 - \frac{P_{[Oe]}}{P_{[e]}} \right|, \quad (\text{S23c})$$

$$R_2(x, y) = \frac{\sum_s P_s P_{Os}}{\sum_s P_s^2} = \frac{\sum_{e \in \mathcal{P}_N} p_e P_{[Oe]}}{\sum_{e \in \mathcal{P}_N} p_e P_{[e]}}. \quad (\text{S23d})$$

Note in particular that $R_1(x, y)$ exactly agrees with the fidelity correlator $F(x, y)$.

In the context of locally decohered stabilizer states [16–19, 21–23, 25–28, 30, 31, 33, 36, 44, 45], where the stabilizer generators g_a are local and the Pauli channel \mathcal{E} is a product of local error channels, the quantities P_s can be understood as partition functions of disordered statistical mechanics models. Each possible error e yields a disorder realization with probability p_e , but the partition function $P_{[e]}$ depends only on the equivalence class of e . The fact that $P_s = \sum_{e \in s} p_e$ is given by a sum over the disorder realization probabilities leads to a “Nishimori”-like condition, i.e., a relation between parameters in the effective disordered statistical mechanics model and the parameters generating its disorder. In this interpretation, it is crucial to note that each of the quantities (S22), (S23a), (S23b), and (S23c) are “quenched” averages, while the Rényi-2 correlator (S23d) is given by an “annealed” average. This observation suggests that the first three observables are likely to all exhibit the same critical phenomena and provide equivalent probes of SWSSB in reasonably local stabilizer codes under local decoherence, while the Rényi-2 correlator generically exhibits a phase transition at a different location and with a different universality class. This picture is easily verified in the most well-known problems of stabilizer codes under local decoherence [16–19].

B. Gibbs States of Stabilizer Code Hamiltonians

Consider a system of N qubits with a stabilizer code Hamiltonian of the form $H = - \sum_a g_a$, such that each g_a is a Pauli string and $[g_a, g_b] = 0$. Typically the stabilizers g_a in the Hamiltonian are *not* algebraically independent, but are instead chosen as a set of local operators; we need not assume anything about the algebra or locality of operators in H in this section. At finite inverse temperature $\beta < \infty$, the system is described by the following Gibbs state:

$$\rho_\beta := \frac{e^{-\beta H}}{\mathcal{Z}_\beta}, \quad \mathcal{Z}_\beta := \text{tr } e^{-\beta H}. \quad (\text{S24})$$

In this state, the canonical purification $|\sqrt{\rho_\beta}\rangle\rangle$ is well-known as the *thermofield double* (TFD) state. Such states can be prepared with relative efficiency in quantum simulators using variational quantum simulation [74–78], and in numerical simulations of tensor network states using time-evolving block decimation (TEBD) [82].

Once again, let us assume that $O \equiv O_x O_y^\dagger$ is a Pauli operator for simplicity. We can then show once again that the Rényi-1 correlator and the fidelity correlator are equal in the Gibbs state ρ_β . First note that if O commutes with H , then $R_1(x, y) = F(x, y) = 1$. More generally, if O anticommutes with a stabilizer g_a , then we have the following identity:

$$O e^{\beta g_a/2} O^\dagger e^{\beta g_a/2} = e^{\beta(O g_a O^\dagger)/2} e^{\beta g_a/2} = e^{-\beta g_a/2} e^{\beta g_a/2} = 1. \quad (\text{S25})$$

Using this observation, one easily computes both the Rényi-1 correlator and the fidelity correlator:

$$R_1(x, y) = F(x, y) = \frac{1}{\mathcal{Z}_\beta} \text{tr} \exp \left\{ \beta \sum_a J_a^O g_a \right\}, \quad J_a^O = \begin{cases} 1, & [O, g_a] = 0 \\ 0, & \{O, g_a\} = 0 \end{cases}. \quad (\text{S26})$$

In other words, both observables can be understood as a type of disorder operator which eliminates stabilizers in H which fail to commute with O . Formal expressions for the other three observables $\mathcal{D}(x, y)$, $D_1(x, y)$, and $R_2(x, y)$ can be computed similarly.

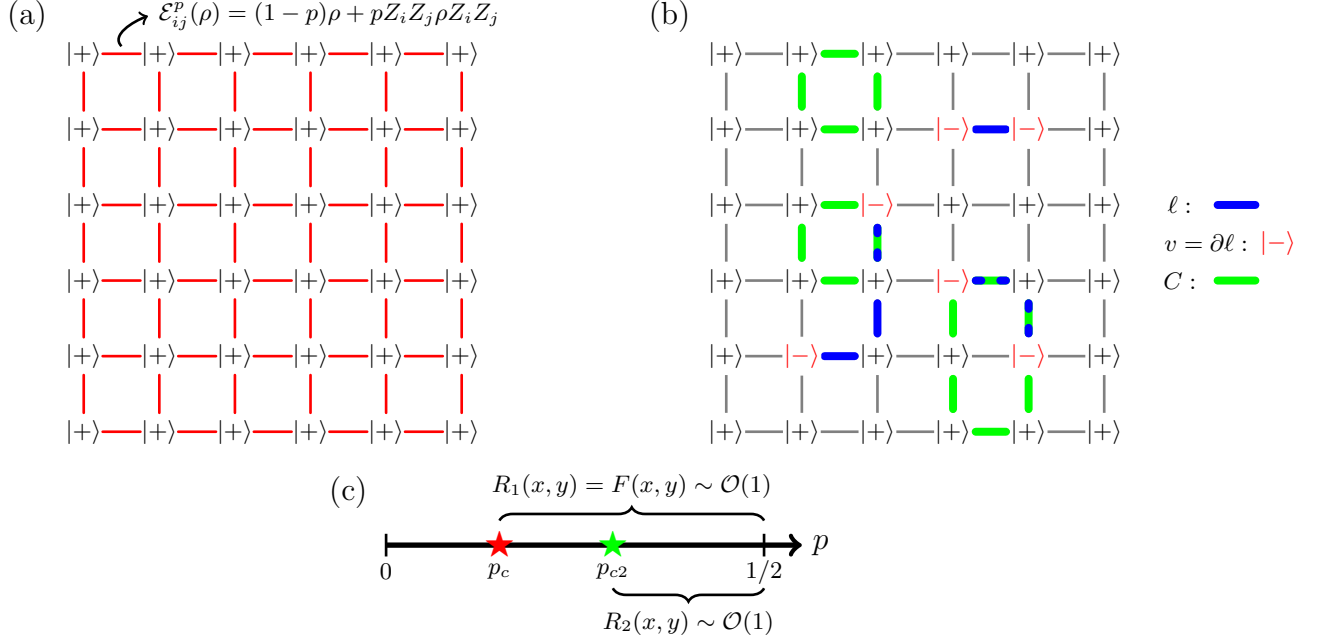


FIG. S1. Schematic depiction of the decohered quantum Ising model and its statistical physics mapping. (a) Starting from an array of qubits in a d -dimensional square lattice, each initialized in the state $|+\rangle$, we apply the dephasing channel \mathcal{E}_{ij}^p to each nearest-neighbor pair $\langle ij \rangle$ of qubits. (b) As in Eq. (S28), the resulting density matrix ρ_p can be unraveled into a sum over “error chains” ℓ , corresponding to a collection of links in the lattice (blue). Each such error chain arises with probability $p_\ell = (1-p)^{dN-|\ell|}p^{|\ell|}$, and results in a set of phase flips at the collection of sites $v = \partial\ell$ (red). The total probability of achieving the “syndrome” v is computed by summing over all error chains with boundary v ; each such error chain can be achieved by adding a closed loop C (green) to an initial representative error ℓ . (c) Phase diagram for the various observables (S9), (S10), and (S17) in the state ρ_p , as a function of p . The Rényi-1 and fidelity correlators exhibit LRO above p_c , while the Rényi-2 correlator exhibits LRO only above p_{c2} . As shown in Ref. [44], all states with $p > p_c$ are two-way connected by short-depth symmetric channels, while a stability theorem forbids the two-way connectivity between states with $p < p_c$ and $p > p_c$. Note that for $d = 1$, $p_c = p_{c2} = 1/2$.

SIV. STRONG-TO-WEAK SPONTANEOUS SYMMETRY-BREAKING IN THE DECOHERED QUANTUM ISING MODEL

In this Appendix we review the decohered quantum Ising model, a paradigmatic example of SWSSB [19, 44, 45]. Our purpose here is to demonstrate how the Rényi-1 correlator (S9) and fidelity correlator (S10) [as well as the other observables (S15), (S16), and (S17)] can all be efficiently mapped to correlation functions in an effective statistical mechanics model using the formalism of Appendix SIII A, *without* the replica trick.

We consider N qubits arranged in a d -dimensional square lattice, with periodic boundary conditions for concreteness. The system is initialized in the pure \mathbb{Z}_2 -symmetric product state $\rho_0 = |+\rangle\langle+|^{\otimes N}$, where $|+\rangle \equiv \frac{1}{\sqrt{2}}(|0\rangle + |1\rangle)$ is the $+1$ eigenstate of the Pauli- X operator. We then subject each nearest-neighbor pair of qubits to a ZZ dephasing channel⁵ of strength p [see Fig. S1(a)]:

$$\mathcal{E}^p = \prod_{\langle ij \rangle} \mathcal{E}_{ij}^p, \quad \mathcal{E}_{ij}^p(\rho) = (1-p)\rho + pZ_iZ_j\rho Z_iZ_j. \quad (\text{S27})$$

This quantum channel is strongly \mathbb{Z}_2 -symmetric, in the sense that each Kraus operator commutes with the parity operator $\Pi = \prod_j X_j$. As a result, the decohered state $\rho_p := \mathcal{E}^p(\rho)$ remains strongly symmetric for all values of p . Nevertheless, we shall show that ρ_p *spontaneously* breaks this strong symmetry down to a residual weak symmetry for sufficiently large p . In $d = 1$ dimension, SWSSB only occurs exactly at the maximal value⁶ $p = 1/2$, while for

⁵ Note that in dimension $d = 2$, this problem is exactly the Wegner dual of the toric code decohered by bit-flip errors. The duality is identified by the operator replacements $Z_iZ_j \rightarrow X_{ab}$ and $X_j \rightarrow B_p$, where ab is a nearest-neighbor pair of sites on the dual lattice bisected by ij , and B_p is the toric code plaquette operator at the plaquette p of the dual lattice centered on the site j of the direct lattice. It should therefore be unsurprising that the SWSSB transition in this setting is described by a random-bond Ising model on the Nishimori line.

$d \geq 2$ there is a stable SWSSB phase.

In the language of Appendix [SIII A](#), we can think of each error e in the channel [\(S18\)](#) with nonzero probability p_e as specified by collection of links ℓ in the lattice (i.e., a ‘1-chain’), visualized as a graph of open strings [see Fig. [S1\(b\)](#)]. Each nearest-neighbor link $\langle ij \rangle$ is included in the graph with probability p , and excluded with probability $1 - p$. Phase-flip errors Z_j are applied at the endpoints of each included link, and since such errors cancel in even multiples, a given graph ℓ applies phase flips only at the collection of its endpoints $v = \partial\ell$ (i.e., a ‘0-chain’). Thus, each equivalence class s of Appendix [SIII A](#) is labeled in this setting by the collection v of vertices on which the error acts nontrivially. The general formulae [\(S18\)](#) and [\(S19\)](#) are therefore specialized to the present context as follows:

$$\begin{aligned} \rho_p &:= \mathcal{E}^p(\rho_0) = \sum_{\ell} p_{\ell} |\partial\ell\rangle\langle\partial\ell|, \quad p_{\ell} := (1-p)^{dN-|\ell|} p^{|\ell|}, \quad |\partial\ell\rangle := \prod_{j \in \partial\ell} Z_j |+\rangle^{\otimes N}, \\ &= \sum_v P_v |v\rangle\langle v|, \quad P_v := \sum_{\ell: \partial\ell=v} p_{\ell}, \quad |v\rangle := \prod_{j \in v} Z_j |+\rangle^{\otimes N}. \end{aligned} \quad (\text{S28})$$

In the above, each state $|v\rangle$ is simply a \mathbb{Z}_2 -even product state in the X basis, and P_v is the total probability of achieving the state $|v\rangle$ by a sequence of phase-flip errors.

As a first observation, note that $\langle v|Z_x Z_y|v\rangle = 0$ for any $x \neq y$, and so ordinary correlation functions of the form $\text{tr}[Z_x Z_y \rho_p]$ trivially have zero correlation length at all values of p . On the other hand, correlation functions such as the Rényi-1 and fidelity correlators can exhibit nontrivial behavior as a function of p [see Fig. [S1\(c\)](#)]. Specifically, the general results from Appendix [SIII A](#) give

$$R_1(x, y) = F(x, y) = \sum_{\ell} p_{\ell} \sqrt{\frac{P_{\partial\ell \oplus \{xy\}}}{P_{\partial\ell}}}, \quad (\text{S29})$$

where \oplus denotes the mod-two union of the sets of vertices $\partial\ell$ and $\{xy\}$, i.e., $\partial\ell \oplus \{xy\} = \partial\ell \cup \{xy\} - \partial\ell \cap \{xy\}$. The form of the other correlators can be written down similarly; we focus on R_1 and F for purposes of clarity. The probability P_v for fixed v can be computed by starting with a fixed representative error ℓ_v which achieves this state (i.e., $v = \partial\ell_v$), and then summing over all other errors $\ell = \ell_v \oplus C$ which differ from the open string ℓ_v by a closed loop C [see Fig. [S1\(b\)](#)]:

$$P_v = (1-p)^{dN} \sum_{C: \partial C=0} \left(\frac{p}{1-p} \right)^{|\ell_v \oplus C|}, \quad (\text{S30})$$

where $\ell_v \oplus C$ denotes the mod-two union of ℓ_v and C , giving another open string with the same endpoints. Clearly, the sum on the right-hand side is independent of the choice of representative ℓ_v . We can now proceed to represent P_v as the partition function of a classical statistical physics model in two distinct ways:

1. The first approach is to regard the sum over closed loops as a *high-temperature expansion*. This approach has the benefit of treating the models in each spatial dimension d on exactly the same footing: as we shall see, P_v is the partition function of a bond-disordered Ising model in d dimensions (more accurately, a disordered $O(1)$ loop model), and the correlation functions $R_1(x, y)$ and $F(x, y)$ are related to two-point correlation functions averaged over quenched disorder. A potential downside of this approach is that the individual Boltzmann weights of P_v are not all positive in this representation, and therefore not of the form $e^{-\beta H}$ for some classical Hamiltonian H .
2. The second approach is to treat the sum over closed loops as a *low-temperature expansion*. For general dimensions $d \geq 2$, the resulting statistical mechanics model is a disordered version of Wegner’s model⁷ $M_{d,d-1}$ [83]; $d = 2$ reproduces the random-bond Ising model on the Nishimori line, while $d = 3$ gives a random-plaquette \mathbb{Z}_2 lattice gauge theory with a similar Nishimori-like condition [16, 84]. These models have previously been studied numerically in detail, and their critical points are known. In this representation, R_1 and F are related to *disorder parameter* correlations, i.e., ratios of partition functions with different disorder realizations.

⁶ For $p > 1/2$, we can rewrite $\mathcal{E}_{ij}^p(\rho) = \mathcal{E}_{ij}^{1-p}(Z_i Z_j \rho Z_i Z_j)$ as a unitary rotation, followed by the same channel at strength $1 - p$. The total channel \mathcal{E}^p does not even require this unitary, i.e., $\mathcal{E}^p = \mathcal{E}^{1-p}$.

⁷ Recall that Wegner’s model $M_{d,k}$ is a classical d -dimensional lattice spin model with Ising spins on unit $(k-1)$ -cells of a hypercubic lattice, with interaction terms in the Hamiltonian taken as the product of all spins belonging to a unit k -cell; 0-cells denote vertices, 1-cells denote links, 2-cells denote plaquettes, and so on. In other words, $M_{d,1}$ for $d \geq 1$ is the ferromagnetic Ising model in d dimensions, with spins on vertices and interactions along links of the lattice; $M_{d,2}$ for $d \geq 2$ is the \mathbb{Z}_2 lattice gauge theory in d dimensions, with spins on links and interactions on plaquettes; and so on. Wegner’s general result was the duality relation between models $M_{d,k}$ and $M_{d,d-k}$, which includes the Kramers-Wannier self-duality of the Ising model in $d = 2$ dimensions, as well as the duality between the Ising model and the \mathbb{Z}_2 lattice gauge theory in $d = 3$ dimensions.

We shall now treat both the low-temperature and high-temperature approaches in turn. The two approaches yield statistical physics models which are dual to each other, providing complementary insight on the SWSSB transition in the density matrix ρ_p .

A. High-Temperature Expansion

Our first method of representing P_v as a classical statistical physics model is to consider the closed loops C as arising from a high-temperature expansion of an Ising system. In other words, we place a classical Ising spin $\sigma_j = \pm 1$ on each site of the lattice, and represent P_v as the following partition function with quenched disorder:

$$P_v = \frac{(1-p)^{dN}}{2^N} \left(\frac{p}{1-p} \right)^{|\ell_v|} \sum_{\{\sigma\}} \prod_{\langle ij \rangle} (1 + t_{ij} \sigma_i \sigma_j), \quad t_{ij} = \begin{cases} p/(1-p), & \langle ij \rangle \notin \ell_v \\ (1-p)/p, & \langle ij \rangle \in \ell_v \end{cases}. \quad (\text{S31})$$

A high-temperature expansion of the above partition function sum then yields a sum over graphs of closed loops in the lattice, with a factor t_{ij} for each link $\langle ij \rangle$ included in a graph. In this representation, independence of the choice of representative ℓ_v follows from inserting $1 = \prod_{\langle ij \rangle \in C} \sigma_i \sigma_j$ for a closed curve C into the Boltzmann weight, which modifies the bonds along the curve C as follows:

$$\begin{aligned} \prod_{\langle ij \rangle \in C} (1 + t_{ij} \sigma_i \sigma_j) &= \left(\prod_{\langle ij \rangle \in C} \sigma_i \sigma_j \right) \left(\prod_{\langle ij \rangle \in C} (1 + t_{ij} \sigma_i \sigma_j) \right) = \prod_{\langle ij \rangle \in C} (\sigma_i \sigma_j + t_{ij}) \\ &= \left(\prod_{\langle ij \rangle \in C} t_{ij} \right) \left(\prod_{\langle ij \rangle \in C} (1 + t_{ij}^{-1} \sigma_i \sigma_j) \right). \end{aligned} \quad (\text{S32})$$

The factor $\prod_{\langle ij \rangle \in C} t_{ij}$ then combines with the prefactor $[p/(1-p)]^{|\ell_v|}$ to give $[p/(1-p)]^{|\ell_v \oplus C|}$. By a similar calculation, inserting a factor $\sigma_x \sigma_y = \prod_{\langle ij \rangle \in \gamma} \sigma_i \sigma_j$ for an *open* string γ with endpoints x and y gives the following result for two-point correlations in this model:

$$\langle \sigma_x \sigma_y \rangle_{\ell_v} := \frac{\sum_{\{\sigma\}} \sigma_x \sigma_y \prod_{\langle ij \rangle} (1 + t_{ij} \sigma_i \sigma_j)}{\sum_{\{\sigma\}} \prod_{\langle ij \rangle} (1 + t_{ij} \sigma_i \sigma_j)} = \frac{P_{v \oplus \{xy\}}}{P_v}. \quad (\text{S33})$$

From Eq. (S29), we immediately obtain the following result for the Rényi-1 correlator and the fidelity correlator:

$$R_1(x, y) = F(x, y) = \sum_{\ell} p_{\ell} \sqrt{\frac{P_{\partial \ell \oplus \{xy\}}}{P_{\partial \ell}}} = \sum_{\ell} p_{\ell} \sqrt{\langle \sigma_x \sigma_y \rangle_{\ell}}. \quad (\text{S34})$$

In the final expression, we can regard the average over ℓ as a simple quenched disorder average in the effective statistical mechanics model, with the value of each nearest-neighbor coupling t_{ij} sampled independently. Note that the magnitude of t_{ij} is a function of the bond disorder probability p , providing a “Nishimori-like” condition. As we will see below, the $d = 2$ model is exactly the Kramers-Wannier dual of the random-bond Ising model on the Nishimori line.

The partition function (S31) is best interpreted as a disordered $O(1)$ loop model on the square lattice; strictly speaking, it is not an Ising model with Boltzmann weights of the form $e^{-\beta H}$, since t_{ij} can be greater than one. Nevertheless, the qualitative phase diagram and the behavior of R_1 and F can easily be determined from this mapping. For small p the model is in a paramagnetic phase, and correlations $\langle \sigma_x \sigma_y \rangle_{\ell}$ decay exponentially in $|x - y|$ for typical realizations of ℓ . On the other hand, for sufficiently large p and in dimensions $d \geq 2$, the model is expected to exhibit a ferromagnetic phase with long-range order, and R_1 and F asymptotically give the disorder-averaged order parameter $\sum_{\ell} p_{\ell} |\langle \sigma \rangle_{\ell}|$ as $|x - y| \rightarrow \infty$. We thus expect a SWSSB transition in ρ_p as a function of p for spatial dimensions $d \geq 2$.

In the case $d = 1$ we can compute R_1 and F exactly in the thermodynamic limit $N \rightarrow \infty$, allowing for us to verify that ρ_p exhibits SWSSB only at $p = 1/2$. For the correlation function, we have

$$\langle \sigma_0 \sigma_r \rangle_{\ell} = \frac{\prod_{j=1}^r t_{j,j+1} + \prod_{j=r+1}^N t_{j,j+1}}{1 + \prod_{j=1}^N t_{j,j+1}} \xrightarrow{r \rightarrow \infty} \prod_{j=1}^r t_{j,j+1} \quad (d = 1), \quad (\text{S35})$$

where we've kept only the leading term as $r \rightarrow \infty$. After taking the square root, the disorder average over each bond variable $\sqrt{t_{j,j+1}}$ can be performed independently. We therefore find the final result

$$R_1(x, y) = F(x, y) \stackrel{r \rightarrow \infty}{\simeq} \left[(1-p) \sqrt{\frac{p}{1-p}} + p \sqrt{\frac{1-p}{p}} \right]^{|x-y|} = \left[2\sqrt{p(1-p)} \right]^{|x-y|} \quad (d=1), \quad (\text{S36})$$

which exhibits exponential decay in $|x-y|$ for all $p < 1/2$. At exactly $p = 1/2$, it is clear that we have perfect long-range order in $\langle \sigma_x \sigma_y \rangle_\ell$ and SWSSB in ρ_p : indeed, the partition function (S31) becomes that of a clean zero-temperature Ising model.

B. Low-Temperature Expansion

To gain further insight on the models in dimensions $d \geq 2$, it is useful to instead treat the sum over closed loops in Eq. (S30) as a low-temperature expansion. This gives a statistical physics model which is dual to the one described in the previous section. A benefit of this approach is that it yields a proper disordered Hamiltonian model, with positive Boltzmann weights of the form $e^{-\beta H}$; in principle this makes the phases of ρ_p easier to interpret, although the models are somewhat baroque in dimensions above $d > 3$. For this reason, rather than working abstractly in general dimensions d , it is useful here to focus on the concrete examples $d = 2, 3$ in turn. We shall simply state the general result that the partition function P_v is described in a low-temperature expansion as a disordered version of the Wegner model $M_{d,d-1}$ [83].

d = 2: Random-Bond Ising Model on the Nishimori Line

Let us first concentrate on the simpler case $d = 2$. Here we think of the sum over closed loops in Eq. (S30) as a sum over one-dimensional domain walls of Ising variables. If we momentarily neglect non-contractible loops in this sum, then we can write each closed loop C as ∂R , the boundary of a two-dimensional set of plaquettes R (i.e., a ‘2-chain’). We can sum over all such collections of plaquettes by placing an Ising spin μ_a at the center of each plaquette a , with $\mu_a = +1$ ($\mu_a = -1$) denoting the exclusion (inclusion) of the plaquette a in R . The boundaries of the region R are then simply given by the bonds $\langle ab \rangle$ in the dual lattice for which $\mu_a \mu_b = -1$. With this notation in mind, we have the following:

$$\begin{aligned} \sum_{C: C=\partial R} \left(\frac{p}{1-p} \right)^{|\ell_v \oplus C|} &= \frac{1}{2} \sum_R \left(\frac{p}{1-p} \right)^{|\ell_v \oplus \partial R|} = \frac{1}{2} \sum_{\{\mu\}} \prod_{\langle ab \rangle} \left(\frac{p}{1-p} \right)^{(1-\eta_{ab} \mu_a \mu_b)/2} \\ &= \frac{1}{2} \left(\frac{p}{1-p} \right)^N \sum_{\{\mu\}} \exp \left\{ J \sum_{\langle ab \rangle} \eta_{ab} \mu_a \mu_b \right\}, \end{aligned} \quad (\text{S37})$$

where we have introduced the bond disorder variable $\eta_{ab} = \pm 1$ and the bond strength J , defined respectively by

$$\eta_{ab} = \begin{cases} +1, & \langle ab \rangle \notin \ell_v \\ -1, & \langle ab \rangle \in \ell_v \end{cases}, \quad e^{-2J} = \frac{p}{1-p}. \quad (\text{S38})$$

The above is simply the partition function of a random-bond Ising model (RBIM) along the Nishimori line. The expression $\eta_{ab} \mu_a \mu_b = \pm 1$ simply counts whether the direct-lattice link bisected by the dual-lattice link $\langle ab \rangle$ is included in $\ell_v \oplus \partial R$ an even ($\eta_{ab} \mu_a \mu_b = +1$) or odd ($\eta_{ab} \mu_a \mu_b = -1$) number of times.

To obtain the full expression for P_v , we must also allow for topologically nontrivial loops C . This is effectively implemented by summing over both periodic and antiperiodic boundary conditions in both spatial directions. More precisely, we define a pair of non-contractible loops Γ_x and Γ_y which encircle the two cycles of the torus, and perform

the sum as follows:

$$\begin{aligned}
\sum_{C:\partial C=0} \left(\frac{p}{1-p}\right)^{|\ell_v \oplus C|} &= \sum_{C:C=\partial R} \left[\left(\frac{p}{1-p}\right)^{|\ell_v \oplus C|} + \left(\frac{p}{1-p}\right)^{|\ell_v \oplus C \oplus \Gamma_x|} + \left(\frac{p}{1-p}\right)^{|\ell_v \oplus C \oplus \Gamma_y|} + \left(\frac{p}{1-p}\right)^{|\ell_v \oplus C \oplus \Gamma_x \oplus \Gamma_y|} \right] \\
&= \frac{1}{2} \left(\frac{p}{1-p}\right)^N \sum_{\{\mu\}} \left[e^{J \sum_{\langle ab \rangle} \eta_{ab} \mu_a \mu_b} + e^{J \sum_{\langle ab \rangle} \eta_{ab}^{(x)} \mu_a \mu_b} + e^{J \sum_{\langle ab \rangle} \eta_{ab}^{(y)} \mu_a \mu_b} + e^{J \sum_{\langle ab \rangle} \eta_{ab}^{(xy)} \mu_a \mu_b} \right] \\
&\equiv \frac{1}{2} \left(\frac{p}{1-p}\right)^N \sum'_{\{\mu\}} e^{J \sum_{\langle ab \rangle} \eta_{ab} \mu_a \mu_b}.
\end{aligned} \tag{S39}$$

Here $\eta_{ab}^{(x)}$, $\eta_{ab}^{(y)}$, and $\eta_{ab}^{(xy)}$ are bond disorder configurations with additional ‘fluxes’ inserted through the holes of the torus; i.e., they are given by the same expression as η_{ab} in Eq. (S38), but with ℓ_v replaced with $\ell_v \oplus \Gamma_x$, $\ell_v \oplus \Gamma_y$, and $\ell_v \oplus \Gamma_x \oplus \Gamma_y$ respectively. Since this technical complication of summing over non-contractible cycles will not matter for any thermodynamic properties, we have hidden it in the final expression, where we use the primed sum to denote an additional sum over periodic and antiperiodic boundary conditions. With these comments in mind, the probabilities P_v in the $d = 2$ dimensional model are given by the following partition function sum:

$$P_v = \frac{1}{2} [p(1-p)]^N \sum'_{\{\mu\}} \exp \left\{ J \sum_{\langle ab \rangle} \eta_{ab} \mu_a \mu_b \right\}. \tag{S40}$$

The original expression for $P_v = \sum_{\ell:\partial\ell=v} p_\ell$ is obtained by performing a low-temperature expansion of the above partition function, i.e., an ordinary sum over domain-wall configurations of the μ_a spins. If we regard a dual-lattice link $\langle ab \rangle$ along which $\eta_{ab} \mu_a \mu_b = -1$ as detecting a segment of domain wall along the direct lattice, then the low-temperature expansion of P_v consists of a sum over *open-string* domain walls. The endpoints of these open strings are “Ising fluxes”, that is, dual-lattice plaquettes $[abcd]$ for which $\eta_{ab} \eta_{bc} \eta_{cd} \eta_{da} = -1$; from Eq. (S38), these are precisely the set of points v in the direct lattice. Finally, the independence of the choice of representative ℓ_v arises from the invariance of P_v under the “gauge transformation” $\eta_{ab} \rightarrow \tau_a \eta_{ab} \tau_b$ for a set of numbers $\tau_a = \pm 1$, which can be compensated by the change of variables $\mu_a \rightarrow \tau_a \mu_a$ in the partition function sum.

From Eq. (S29), the Rényi-1 and fidelity correlators are related to the ratio of partition functions $P_{v \oplus \{xy\}}/P_v$. We found in Eq. (S33) that this quantity was given by the two-point correlation function $\langle \sigma_x \sigma_y \rangle_{\ell_v}$ in terms of the σ_j degrees of freedom. In the μ_a degrees of freedom, this ratio takes the form of a *disorder parameter* correlation function, in which we compute the free energy cost of inserting an extra pair of Ising fluxes at the dual lattice plaquettes x and y . Explicitly, we consider a curve γ through the direct lattice (i.e., the dual of the dual lattice) with endpoints at sites x and y , and flip the sign of the bond disorder variables η_{ab} along each dual-lattice bond $\langle ab \rangle$ bisected by γ . This is equivalent to modifying the disorder realization ℓ_v to $\ell_v \oplus \gamma$. The ratio of the resulting partition function to the original one defines the disorder parameter correlation function:

$$\frac{P_{v \oplus \{xy\}}}{P_v} = \frac{\sum'_{\{\mu\}} \exp \left\{ J \sum_{\langle ab \rangle} \tilde{\eta}_{ab} \mu_a \mu_b \right\}}{\sum'_{\{\mu\}} \exp \left\{ J \sum_{\langle ab \rangle} \eta_{ab} \mu_a \mu_b \right\}}, \quad \tilde{\eta}_{ab} = \begin{cases} +\eta_{ab}, & \eta_{ab} \notin \gamma \\ -\eta_{ab}, & \eta_{ab} \in \gamma \end{cases}. \tag{S41}$$

In the large J (small p) phase of the RBIM, the spins μ_a are in a ferromagnetic phase. Modifying the disorder by γ effectively inserts an open-string domain wall from x to y , whose free energy δF grows linearly with the separation $|x - y|$. The above ratio of partition functions can be interpreted as $e^{-\delta F}$, and so $P_{v \oplus \{xy\}}/P_v$ decays exponentially in $|x - y|$ for typical disorder realizations. On the other hand, in the small J (large p) phase, the μ_a spins are in a paramagnetic phase, and it costs an order-one free energy to insert such a domain wall into the system. Consequently, $P_{v \oplus \{xy\}}/P_v$ is of order unity in typical realizations, leading to long-range order in the correlators (S29). We thus recover the same qualitative phase diagram as we found in Sec. SIV A: at some critical dephasing strength p_c , we expect a phase transition to a SWSSB phase above which the Rényi-1 and fidelity correlators become long-range ordered.

The true benefit of the above RBIM representation of P_v is the vast literature available on the critical phenomena of the RBIM on the Nishimori line. For example, we can immediately conclude that the critical value of p above which the SWSSB phase arises is approximately $p_c \approx 0.109$ [85].

d = 3: Random-Plaquette \mathbb{Z}_2 Gauge Theory

In $d = 3$ dimensions, we interpret the sum over closed loops in Eq. (S30) as a sum over flux tubes in a \mathbb{Z}_2 gauge theory. Let us once again neglect non-contractible loops for the moment and regard closed loops C as the boundary of a 2-chain R , which should be pictured as a collection of plaquettes in the direct lattice. To enumerate all such choices, we place an Ising spin μ_{ab} at the center of each nearest-neighbor link $\langle ab \rangle$ of the dual lattice, which passes directly through a plaquette of the direct lattice. We set $\mu_{ab} = +1$ ($\mu_{ab} = -1$) whenever the plaquette pierced by $\langle ab \rangle$ is included (excluded) in R . The boundaries of R are then found by taking the product of spins μ_{ab} around a dual-lattice plaquette; this product is $+1$ (-1) whenever the direct-lattice edge which pierces the dual-lattice plaquette belongs to ∂R . Thus, we obtain the following representation of the sum over closed loops:

$$\begin{aligned} \sum_{C: C=\partial R} \left(\frac{p}{1-p} \right)^{|\ell_v \oplus C|} &= \frac{1}{2^N} \sum_R \left(\frac{p}{1-p} \right)^{|\ell_v \oplus \partial R|} = \frac{1}{2^N} \sum_{\{\mu\}} \prod_{[abcd]} \left(\frac{p}{1-p} \right)^{(1-\eta_{abcd}\mu_{ab}\mu_{bc}\mu_{cd}\mu_{da})/2} \\ &= \frac{1}{2^N} \left(\frac{p}{1-p} \right)^{3N/2} \sum_{\{\mu\}} \exp \left\{ J \sum_{[abcd]} \eta_{abcd} \mu_{ab} \mu_{bc} \mu_{cd} \mu_{da} \right\}. \end{aligned} \quad (\text{S42})$$

This is the partition function of the random-plaquette \mathbb{Z}_2 gauge theory, introduced in Refs. [16, 84]. The coupling constant J satisfies the same Nishimori condition as before; the plaquette disorder variable η_{abcd} tracks whether the dual-lattice plaquette $[abcd]$ is pierced by the links ℓ_v :

$$\eta_{abcd} = \begin{cases} +1, & [abcd] \notin \ell_v \\ -1, & [abcd] \in \ell_v \end{cases}. \quad (\text{S43})$$

Once again, to obtain P_v we must modify this sum to include non-contractible closed loops C ; in the present context, this amounts to allowing odd numbers of non-contractible flux tubes to traverse the periodic boundaries of the system. With analogous primed sum notation to the previous section, P_v is now given by

$$P_v = \frac{1}{2^N} [p(1-p)]^{3N/2} \sum'_{\{\mu\}} \exp \left\{ J \sum_{[abcd]} \eta_{abcd} \mu_{ab} \mu_{bc} \mu_{cd} \mu_{da} \right\}. \quad (\text{S44})$$

As before, the original form of P_v is recovered by performing a low-temperature expansion of the above partition function sum. If we regard the dual-lattice plaquettes $[abcd]$ for which $\eta_{abcd}\mu_{ab}\mu_{bc}\mu_{cd}\mu_{da} = -1$ as containing \mathbb{Z}_2 gauge flux, then the low-temperature expansion of P_v consists of a sum over open-string flux tubes. The endpoints of these flux tubes are “magnetic monopoles”, i.e., cubes \mathcal{C} in the dual lattice (centered on sites of the direct lattice) for which $\prod_{[abcd] \in \mathcal{C}} \eta_{abcd} = -1$. From Eq. (S43), these monopoles lie at precisely the sites v of the error syndromes in the direct lattice. Finally, the independence of the choice of representative ℓ_v arises from the invariance of P_v under the “higher-form” gauge transformation $\eta_{abcd} \rightarrow \tau_{ab}\tau_{bc}\tau_{cd}\tau_{da}\eta_{abcd}$ for some set of numbers $\tau_{ab} = \pm 1$ on each link of the dual lattice; this transformation can be compensated by the change of variables $\mu_{ab} \rightarrow \tau_{ab}\mu_{ab}$ in the partition function sum.

Just as in the $d = 2$ case, the correlation function $\langle \sigma_x \sigma_y \rangle_\ell = P_{\partial\ell + \{xy\}} / P_{\partial\ell}$ maps to a disorder parameter correlation function in the above dual representation. In the three-dimensional case, this corresponds to the free energy cost of inserting two extra magnetic monopoles at the cubes centered on x and y . For large J (small p) the lattice gauge theory is in a deconfined phase, and magnetic flux is expelled; consequently, the flux tube costs a free energy linear in its length, and $\langle \sigma_x \sigma_y \rangle_\ell$ decays exponentially in $|x - y|$ for typical realizations of ℓ . On the other hand, for small J (large p) the lattice is in a confined phase, and flux tubes are proliferated. Inserting two far-separated extra monopoles therefore costs an order-one free energy, and $\langle \sigma_x \sigma_y \rangle_\ell$ is typically of order-one as $|x - y| \rightarrow \infty$. We therefore once again recover the qualitative phase diagram predicted in Sec. SIV A: at some critical dephasing strength p_c , we expect a SWSSB phase transition above which the Rényi-1 and fidelity correlators become long-range ordered.

Once again, the critical phenomena of the \mathbb{Z}_2 random-plaquette gauge theory has been studied extensively in connection to error thresholds in surface codes [16, 84, 86]. For example, numerical simulations indicate a critical error rate of $p_c \approx 0.033$ [86].

C. Rényi-2 Correlations and Annealed Averages

We finish by commenting on the behavior of the Rényi-2 correlation function $R_2(x, y)$, defined in Eq. (S17). From the general discussion of Sec. SIII A, we expect that $R_2(x, y)$ will be given by an *annealed* average correlation function rather than a quenched average; correspondingly, it exhibits the critical phenomena of a clean d -dimensional Ising model.

Although R_2 can again be calculated using the formalism of Sec. SIII A, a simpler approach is to expand ρ_0 and ρ_p in the Pauli-Z basis. Using $|+\rangle = \frac{1}{\sqrt{2}}(|0\rangle + |1\rangle)$, we have

$$\begin{aligned} \rho_0 &= \frac{1}{2^N} \sum_{\{\sigma, \sigma'\}} |\{\sigma\}\rangle \langle \{\sigma'\}|, \quad \rho_p = \frac{1}{2^N} \sum_{\{\sigma, \sigma'\}} \prod_{\langle ij \rangle} [(1-p) + p\sigma_i \sigma'_i \sigma_j \sigma'_j] |\{\sigma\}\rangle \langle \{\sigma'\}| \\ &= \frac{1}{2^N} \frac{(1-p)^{dN}}{\cosh^{dN}(\beta/2)} \sum_{\{\sigma, \sigma'\}} \exp \left\{ \frac{\beta}{2} \sum_{\langle ij \rangle} \sigma_i \sigma'_i \sigma_j \sigma'_j \right\} |\{\sigma\}\rangle \langle \{\sigma'\}|, \end{aligned} \quad (\text{S45})$$

where $|\{\sigma\}\rangle = |\sigma_1 \dots \sigma_N\rangle$ is a computational basis state⁸, and β is defined via the relation $\tanh \beta/2 = p/(1-p)$. the purity is therefore given by

$$\text{tr } \rho_p^2 = \left[\frac{1}{2^N} \frac{(1-p)^{dN}}{\cosh^{dN}(\beta/2)} \right]^2 \sum_{\{\sigma, \sigma'\}} \exp \left\{ \beta \sum_{\langle ij \rangle} \sigma_i \sigma'_i \sigma_j \sigma'_j \right\} = \left[\frac{1}{2^N} \frac{(1-p)^{dN}}{\cosh^{dN}(\beta/2)} \right]^2 2^N \sum_{\{\sigma\}} \exp \left\{ \beta \sum_{\langle ij \rangle} \sigma_i \sigma_j \right\}. \quad (\text{S46})$$

In the final expression, we have performed the change of summation variables $\sigma_j \sigma'_j \rightarrow \sigma_j$, after which the $\{\sigma'\}$ summation drops out completely. Thus, the purity $\text{tr } \rho_p^2$ is proportional to the partition function of a d -dimensional Ising model at inverse temperature⁹ β . Meanwhile, the numerator of R_2 is obtained by inserting $Z_x Z_y$ on both sides of one factor of ρ_p , which gives the same expression as above with $\sigma_x \sigma'_x \sigma_y \sigma'_y$ inserted. After the same change of summation variables, this becomes simply $\sigma_x \sigma_y$. We therefore find that R_2 is given simply by the correlation function of a d -dimensional Ising model:

$$R_2(x, y) = \frac{\text{tr}[Z_x Z_y \rho_p Z_x Z_y \rho_p]}{\text{tr } \rho_p^2} = \frac{\sum_{\{\sigma\}} \sigma_x \sigma_y e^{\beta \sum_{\langle ij \rangle} \sigma_i \sigma_j}}{\sum_{\{\sigma\}} e^{\beta \sum_{\langle ij \rangle} \sigma_i \sigma_j}}. \quad (\text{S47})$$

In two dimensions, R_2 exhibits a phase transition at $\beta_{c2} = \frac{1}{2} \log(1 + \sqrt{2})$, corresponding to $p_{c2} \approx 0.178$. Notably, this value is larger than the RBIM critical point which controls the Rényi-1 and fidelity correlators, implying a contiguous region of SWSSB without long-range order in the Rényi-2 correlator. Similarly, the phase transition occurs in three dimensions at $\beta_{c2} \approx 0.221$ [87], corresponding to $p_{c2} \approx 0.099$. This is once again larger than the critical point of the random-plaquette gauge theory.

SV. STRONG-TO-WEAK SPONTANEOUS SYMMETRY BREAKING IN THE ONE-DIMENSIONAL TRANSVERSE-FIELD ISING MODEL AT NONZERO TEMPERATURES

In this section, we demonstrate that the thermal Gibbs state of the one-dimensional transverse-field Ising model (TFIM) exhibits SWSSB at any nonzero temperature. As briefly mentioned in the main text (and discussed in more detail in Ref. [44]), SWSSB is expected to be a generic feature of the symmetry-restored phase of thermal Gibbs states. This is easily verified in the case of commuting projector Hamiltonians. The exact solvability of the one-dimensional TFIM allows us to additionally verify this feature in a simple non-commuting setting.

We consider N qubits in one spatial dimension with periodic boundary conditions. The Hamiltonian is

$$H = -J \sum_{j=1}^N \left\{ Z_j Z_{j+1} + g X_j \right\}, \quad (\text{S48})$$

⁸ Note the abuse of notation: $\sigma = \pm 1$, but $|\sigma = +1\rangle$ corresponds to the state $|0\rangle$ and $|\sigma = -1\rangle$ corresponds to the state $|1\rangle$. One should not get confused, for example, in thinking that σ_j can take the value zero.

⁹ As a sanity check, the limit $p \rightarrow 0$ corresponds to the infinite temperature limit $\beta \rightarrow 0$, which gives $\text{tr } \rho_p^2 = 1$ as desired. On the other hand, the limit $p \rightarrow 1/2$ corresponds to $\beta \rightarrow \infty$, which gives the purity $\text{tr } \rho_p^2 = 2^{-(N-1)}$ as expected.

with $Z_{N+1} \equiv Z_1$. This model exhibits a \mathbb{Z}_2 parity symmetry generated by $\Pi = \prod_{j=1}^N$. Our focus is on observables in the parity-even sector of the thermal Gibbs state, with the density matrix

$$\rho_\beta = \frac{P_\Pi e^{-\beta H}}{\mathcal{Z}_\beta}, \quad \mathcal{Z}_\beta = \text{tr}[P_\Pi e^{-\beta H}], \quad P_\Pi = \frac{1 + \Pi}{2}. \quad (\text{S49})$$

The TFIM is exactly solvable via the Jordan-Wigner transformation. We define the Majorana fermion operators

$$\gamma_{2j-1} = \left[\prod_{i=1}^{j-1} X_i \right] Z_j, \quad \gamma_{2j} = \left[\prod_{i=1}^{j-1} X_i \right] Y_j, \quad (\text{S50})$$

which satisfy the anticommutation relations $\{\gamma_i, \gamma_j\} = 2\delta_{ij}$, as well as the useful identities $X_j = i\gamma_{2j-1}\gamma_{2j}$ and $Z_j Z_{j+1} = i\gamma_{2j}\gamma_{2j+1}$. In terms of the Majoranas, H is written as

$$H = -iJg \sum_{j=1}^N \gamma_{2j-1}\gamma_{2j} - iJ \sum_{j=1}^{N-1} \gamma_{2j}\gamma_{2j+1} + iJ\Pi\gamma_{2N}\gamma_1. \quad (\text{S51})$$

In other words, H is a model of free Majorana fermions with nearest-neighbor couplings of alternating strength. From the last term, we see that the Majorana chain has antiperiodic (periodic) boundary conditions in the parity-even (parity-odd) sector. Since ρ_β is projected into the parity-even sector by design, we may simply set $\Pi = 1$ and use antiperiodic boundary conditions. Our Hamiltonian is therefore a simple quadratic Majorana fermion Hamiltonian, of the general form

$$H = \frac{i}{4} \sum_{i,j=1}^{2N} \gamma_i A_{ij} \gamma_j, \quad (\text{S52})$$

where A is a $2N \times 2N$ real antisymmetric matrix. Arbitrary correlation functions of H can then be efficiently computed numerically for large values of N ; see Appendix A of Ref. [88] for a review.

Our goal is to compute the following Rényi-1 correlator:

$$\begin{aligned} R_1(x, y) &= \text{tr}[Z_x Z_y \sqrt{\rho_\beta} Z_x Z_y \sqrt{\rho_\beta}] \\ &= \frac{1}{\mathcal{Z}_\beta} \text{tr}[P_\Pi Z_x Z_y e^{-\beta H/2} Z_x Z_y e^{-\beta H/2}] \\ &= \frac{1}{\mathcal{Z}_\beta} \text{tr}\left[P_\Pi \left(e^{\beta H/2} Z_x Z_y e^{-\beta H/2}\right) Z_x Z_y e^{-\beta H}\right]. \end{aligned} \quad (\text{S53})$$

In other words, R_1 is simply an imaginary time-ordered four-point correlation function, with two of the operators evolved to imaginary time $\tau = \beta/2$. Before moving onto the general computation, let us compute $R_1(x, y)$ in two extreme limits: deep in the ferromagnetic regime with $g \rightarrow 0$, and deep in the paramagnetic regime $J \rightarrow 0$, $Jg \equiv h = \text{const}$. In the former limit, $Z_x Z_y$ commutes with $\sqrt{\rho_\beta}$, and so we trivially have $R_1(x, y) = 1$. In the latter limit, we can use the result of Sec. [SIII B](#) to immediately obtain $R_1(x, y) = \text{sech}^2(\beta h)$. Thus, we find in both regimes that SWSSB arises at at any nonzero temperature.

We now move onto an efficient numerical free fermion method to compute $R_1(x, y)$ for general values of g . In terms of the Majoranas, the product $Z_x Z_y$ is (assuming $y > x$)

$$Z_x Z_y = i^{(y-x)} \gamma_{2x} \dots \gamma_{2y-1}. \quad (\text{S54})$$

To evolve this product to imaginary time $\beta/2$, we insert factors of $e^{\beta H/2} e^{-\beta H/2}$ between each fermion, and use the identity

$$e^{\tau H} \gamma_i e^{-\tau H} = \sum_j [e^{-iA\tau}]_{ij} \gamma_j, \quad (\text{S55})$$

which follows easily from the Campbell-Baker-Hausdorff formula. Since each $\gamma_i(\tau) \equiv e^{\tau H} \gamma_i e^{-\tau H}$ is simply a linear combination of Majoranas, we can in principle compute the expectation value of any product of Majoranas using Wick's theorem [89]:

$$\begin{aligned} \langle \gamma_{i_1}(\tau_1) \dots \gamma_{i_{2n}}(\tau_{2n}) \rangle_\beta &\equiv \frac{1}{\text{tr} e^{-\beta H}} \text{tr} [\gamma_{i_1}(\tau_1) \dots \gamma_{i_{2n}}(\tau_{2n}) e^{-\beta H}] \\ &= \sum_{\text{Pairings } P} (-1)^{|P|} \langle \gamma_{i_{P(1)}}(\tau_{P(1)}) \gamma_{i_{P(2)}}(\tau_{P(2)}) \rangle_\beta \dots \langle \gamma_{i_{P(2n-1)}}(\tau_{P(2n-1)}) \gamma_{i_{P(2n)}}(\tau_{P(2n)}) \rangle_\beta. \end{aligned} \quad (\text{S56})$$

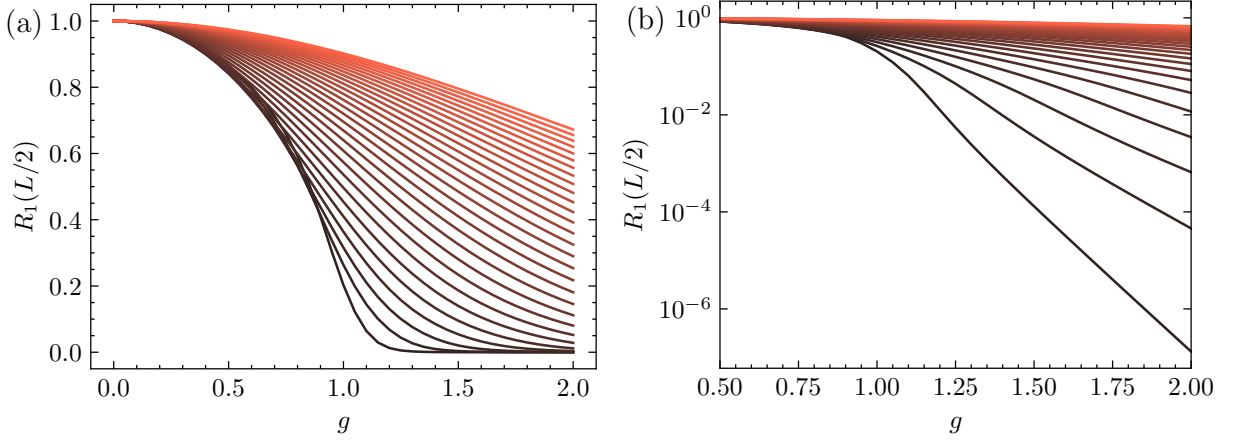


FIG. S2. Numerical results for the Rényi-1 correlator $R_1(x, y)$ for $|x - y| = L/2$ in the finite-temperature Gibbs state of the transverse-field Ising model on L sites; here $L = 128$. Note that the density matrix is restricted to the parity-even sector to achieve a strongly-symmetric density matrix, as in Eq. (S49). Each curve corresponds to a different temperature, in the range $[0.15J, 2.95J]$ in intervals of $0.1J$. Darker colors denote lower temperatures. (a) For very low temperatures, $R_1(x, y)$ exhibits crossover behavior in the vicinity of the zero-temperature transition point $g = 1$; in the limit $T \rightarrow 0$, $R_1(L/2)$ would exactly mimic the behavior of $\langle Z \rangle^4$. As the temperature is raised, the crossover is smoothed further. (b) The same plot as in (a), with the vertical axis on a logarithmic scale. We see that $R_1(L/2)$ decays exponentially in g with a slope set by the inverse temperature, as expected from the $J \rightarrow 0$ analytical solution for $R_1(x, y)$.

Importantly, the expectation values required to compute R_1 are all very high-order expectation values, with a large number of contractions. We can nevertheless compute such expectation values by converting the above sum over pairings into the Pfaffian of a matrix. Explicitly, define an antisymmetric matrix \mathcal{G}_{ab} with $a, b = 1, \dots, 2n$ via $\mathcal{G}_{ab} = -\mathcal{G}_{ba} = \langle \gamma_{i_a}(\tau_a) \gamma_{i_b}(\tau_b) \rangle_\beta$. Then Wick's theorem as written above can be reorganized as follows:

$$\begin{aligned}
 \langle \gamma_{i_1}(\tau_1) \dots \gamma_{i_{2n}}(\tau_{2n}) \rangle_\beta &= \sum_{\text{Pairings } P} (-1)^{|P|} \mathcal{G}_{P(1), P(2)} \dots \mathcal{G}_{P(2n-1), P(2n)} \\
 &= \frac{1}{2^n n!} \sum_{\sigma \in S_{2n}} (-1)^{|\sigma|} \mathcal{G}_{\sigma(1), \sigma(2)} \dots \mathcal{G}_{\sigma(2n-1), \sigma(2n)} \\
 &= \text{Pf}(\mathcal{G}).
 \end{aligned} \tag{S57}$$

The Pfaffian can then be computed efficiently using the algorithm of Ref. [90].

Figure S2 provides our numerical results for the Rényi-1 correlator in the parity-even Gibbs state (S49). For simplicity we work in a system of size $L = 128$ and fix $|x - y| = L/2$; larger system sizes and more detailed numerical studies are easily accessible. Each curve corresponds to a different temperature, with the lowest temperature (darkest black line) given by $T = 0.15J$, while the highest temperature (brightest red line) corresponds to $T = 2.95J$. We see that $R_1(L/2)$ is indeed nonzero for all $T > 0$. Its exponential decay with g at low temperatures is as expected from the analytical solution for $J \rightarrow 0$, with a decay constant proportional to the inverse temperature β . Thus, our numerics support the conclusion that the one-dimensional TFIM exhibits SWSSB at all nonzero temperatures, for all values of g .